*Journal of Statistical Physics, Vol. 49, Nos. 3/4, 1987*

# The Goodness of Ergodic Adiabatic Invariants

**Reggie Brown,[1,2] Edward Ott,[1,2,3] and Celso Grebogi[1]**

*Received March 25, 1987*

For a "slowly" time-dependent Hamiltonian system exhibiting chaotic motion that ergodically covers the energy surface, the phase space volume enclosed inside this surface is an adiabatic invariant. In this paper we examine, both numerically and theoretically, how the error in this "ergodic adiabatic invariant" scales with the slowness of the time variation of the Hamiltonian. It is found that under certain circumstances, the error is diffusive and scales like $T^{-1/2}$, where $T$ is the characteristic time over which the Hamiltonian changes. On the other hand, for other cases (where motion in the Hamiltonian has a long-time $1/t$ tail in a certain correlation function), the error scales like $[T^{-1}\ln(T)]^{1/2}$. Both of these scalings are verified by numerical experiments. In the situation where invariant tori exist amid chaos, the motion may not be fully ergodic on the entire energy surface. The ergodic adiabatic invariant may still be useful in this case and the circumstances under which this is so are investigated numerically (in particular, the islands have to be small enough).

**KEY WORDS:** Ergodicity; time-dependent Hamiltonian; decay of correlations; adiabatic invariant; billiard; chaos.

## 1. INTRODUCTION

We consider a conservative dynamical system characterized by a time-dependent Hamiltonian $H(\mathbf{p}, \mathbf{q}; \varepsilon t)$, where $\mathbf{p}$ and $\mathbf{q}$ are $N$-vectors, and the explicit time dependence of $H$ is "slow." To emphasize this slowness, we have written the third argument of $H$ as $\varepsilon t$, where we shall formally take $\varepsilon$ small. Alternatively, we can set $T=\varepsilon^{-1}$ and think of $T$ as the time scale over which $H(\mathbf{p}, \mathbf{q}; \varepsilon t)$ goes through an order-one change, $T^{-1}\sim$

[1] Laboratory for Plasma and Fusion Energy Studies, University of Maryland, College Park, Maryland 20742.

[2] Department of Physics and Astronomy, University of Maryland, College Park, Maryland 20742.

[3] Department of Electrical Engineering, University of Maryland, College Park, Maryland 20742.



0022-4715/87/1100-0511$05.00/0 

$H^{-1}\,\partial H/\partial t$. The statement that this time dependence is slow (or adiabatic) is equivalent to saying that $T$ is much longer than any relevant characteristic time for the particle motion in the "frozen" Hamiltonian[4] $H(\mathbf{p}, \mathbf{q}; \varepsilon t_0)$, where $t_0$ is a constant.

For the case where motion in the frozen Hamiltonian is periodic,

$$[\mathbf{p}(t), \mathbf{q}(t)] = [\mathbf{p}(t+\tau_p), \mathbf{q}(t+\tau_p)]$$

this situation leads to the well-known adiabatic invariant $\mu = \oint \mathbf{p} \cdot d\mathbf{q}$, where $\oint$ denotes integration over one period $\tau_p$. The adiabatic invariant for periodic motion was discussed by Boltzmann and subsequently by Helmholtz, Hertz, and Rayleigh, among others (cf. Jammer[1] for discussion and primary references). By the assertion that $\mu$ is an adiabatic invariant we mean that a particle orbit approximately conserves $\mu$ over a time interval large enough that $H$ experiences an order-one change provided that this change occurs slowly (in the sense already mentioned). For the case of one degree of freedom ($N=1$) and periodic motion, the conservation of $\mu$ has been shown to be very good[2-4] in that one can define a quantity close to $\mu$ for which the error in the adiabatic approximation is less than $O(\varepsilon^m)$ if $H$ is $m$-times differentiable with respect to $t$. [In fact, in solvable examples[5] it is common for the error to be of the form $\exp(-\kappa/\varepsilon)$.] The utility of the adiabatic invariant for periodic motion has long been recognized. For example, in plasma physics it forms the basis of the fundamental concept of mirror confinement of charged particles[6] and has also been extensively used in performing stability calculations.[7],[5] In addition, in the early theory of quantum mechanics, Ehrenfest[9] argued that $\oint \mathbf{p} \cdot d\mathbf{q}$ was a proper quantity to quantize because it is an adiabatic invariant [e.g., for a harmonic oscillator with frequency $\omega$ and energy $E$, $E/\omega = (n+1/2)\hbar$, quantum mechanically, while $E/\omega$ is an adiabatic invariant of the classical mechanics for slow variation of the oscillation frequency $\omega = \omega(\varepsilon t)$].

Here we shall consider another type of adiabatic invariant. We presume that the number of degrees of freedom is greater than 1, $N>1$, and that motion in the frozen Hamiltonian is chaotic and ergodic on the constant-energy surface, $H(\mathbf{p}(t), \mathbf{q}(t); \varepsilon t_0) = \text{const}$, for all $t_0$ in some range, $t_1 \geqslant t_0 \geqslant 0$. Consequently the motion in the frozen Hamiltonian has no additional isolating constants of the motion other than the frozen Hamiltonian itself. In this case, as shown subsequently, the volume enclosed within the surface of constant $H$ is an adiabatic invariant.[6] (This

[4] By the term "frozen Hamiltonian" we mean the time-independent Hamiltonian $\tilde{H}(\mathbf{p}, \mathbf{q})$ given by $\tilde{H} = H(\mathbf{p}, \mathbf{q}; \varepsilon t_0)$, where $t_0$ is a *constant*.

[5] For a recent example see Antonsen and Lee.[8]

[6] For $N=1$, this reduces to the adiabatic invariant $\oint p\,dq$.

presupposes, of course, that this volume is finite.) This case of an adiabatic invariant for $N \gg 1$ (statistical mechanics) was stated by Boltzmann.[7] The volume inside the constant-$H$ surface is

$$\mu(E, t) \equiv \iint U[E - H(\mathbf{p}, \mathbf{q}; \varepsilon t)]\, d^N p\, d^N q \tag{1}$$

where $U[\cdots]$ denotes the unit step function and $E$ is the energy. Thus, for example, given an initial condition and the corresponding energy $E = E_0$ at $t = 0$, calculation of $\mu(E, t)$ from Eq. (1) allows us to obtain an approximation to the energy $E(t)$ at all subsequent times via $\mu(E, t) = \mu(E_0, 0)$. We call $\mu(E, t)$ for $N > 1$ the *ergodic adiabatic invariant.*[11] To see how the approximate invariance of the quantity given by Eq. (1) follows from Hamilton's equations, we note that if *any* closed surface is specified at $t = 0$ and each point on that surface is evolved, then the new surface must enclose the same phase space volume as the initial surface.[12] If a particle wanders ergodically over the $H(\mathbf{p}, \mathbf{q}; \varepsilon t_0) = E$ surface in a time short compared to $T$, then, as $t$ increases, an ensemble of particles on the initial $H = \text{const}$ surface will all have qualitatively similar trajectories. In particular, their subsequent energies will be approximately equal. Thus, an initial $H = \text{const}$ surface evolves into another surface, which is close to being an $H = \text{const}$ surface (cf. Fig. 1). Hence Eq. (1) is an adiabatic invariant.

[7] For example, a statement within the context of statistical mechanics appears in Ref. 10.

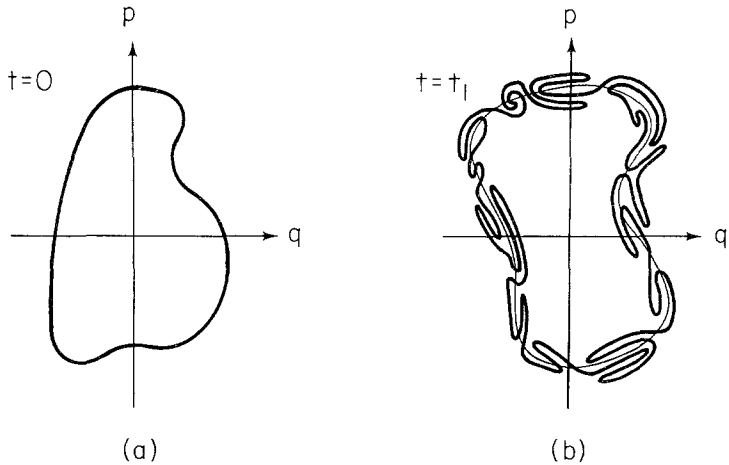


Fig. 1. (a) An initial $H = E$ surface at $t = 0$ evolves under the exact dynamics to (b) a convoluted surface that is close to the surface $H = E(t_1)$, where $E(t_1)$ is obtained from the constancy of $\mu$. The phase space volume inside the initial surface at $t = 0$ and inside the squiggly surface at $t = t_1$ are exactly equal.

With the advent of computer solutions for particle motion, it has become more and more appreciated that low-degree-of-freedom Hamiltonian systems can often behave chaotically in such a way that particle motion samples the surface of constant $H$, if not fully, at least nearly fully. Thus, the ergodic adiabatic invariant is of interest not only for the $N \to \infty$ limit of statistical mechanics, but also for low $N$. This seems to have first been appreciated by Lovelace[13] (who used the $N=2$ ergodic adiabatic invariant to analyze the compression of a plasma ring confined by large-orbit gyrating ions) and Wong *et al.*[14] (who used it in formulating a proposed magnetic plasma confinement concept).

At this point it may be instructive to discuss an example of the ergodic adiabatic invariant. Consider the situation shown in Fig. 2, where a point particle $P$ moves in a two-dimensional square container with impenetrable walls of dimension $L$ in the center of which is situated an impenetrable circular barrier of radius $r$. (The latter may also be thought of as a second large and very massive particle.) The dynamics is specified by the constancy of the particle velocity between encounters with the boundaries and by the law of specular reflection in the local frame moving with the boundary at the point of collision. For the case where the geometry (i.e, $L$ and $r$) is held fixed in time, the motion of $P$ in this "billiard" is known[15] to be chaotic and ergodic on the energy surface. The ergodic adiabatic invariant for a billiard ($N=2$) is $\mu = 2\pi mEA$ (Section 2), where $E = mv^2/2$ and $A$ is the accessible area ($A = L^2 - \pi r^2$ for this example). Thus, for this example, if

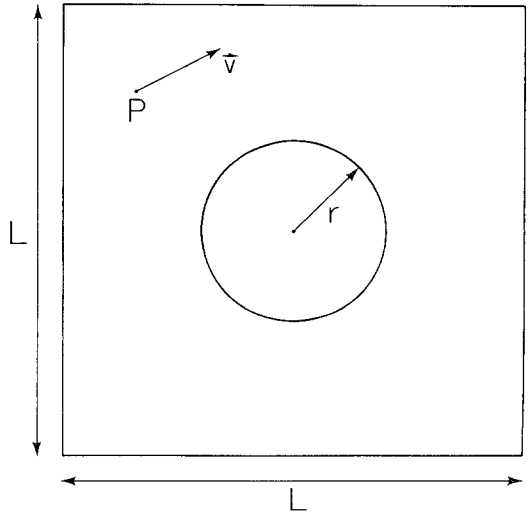


Fig. 2. Square billiard (Example 2).

one of the dimensions, $L$ or $r$, is varied slowly with time, then the variation of $E$ would be determined by the approximate constancy of $\mu$,

$$E(t) \simeq E(0)\, A(0)/A(t) \tag{2}$$

This result also has an intimate connection to the adiabatic gas law $\tilde{p}V^{\gamma} = \text{const}$, where $V$ is the volume, $\gamma = (\tilde{N}+2)/\tilde{N}$, $\tilde{N}$ is the number of degrees of freedom of *each* gas particle, $\tilde{p}$ is the pressure, $\tilde{p} = nk\tilde{T}$ (with $\tilde{T}$ the temperature and $n$ the particle density), and $\tilde{N}k\tilde{T}/2$ is the average energy of a gas particle. Now consider the situation in Fig. 2, and treat it as if it was a gas. Since there the situation is two dimensional, $V = A$. Since there is only one particle, $\tilde{N} = 2$, $\gamma = 2$, $n = 1/A$, and $k\tilde{T} = E$. Thus, $\tilde{p}V^{\gamma} = EA$, so that constancy of $\tilde{p}V^{\gamma}$ implies constancy of $EA$ and therefore $\mu$. Hence, the single chaotic particle behaves like a gas. [For the three-dimensional case where Fig. 2 illustrates a sphere inside a cube, $\tilde{N} = 3$, $n = 1/V$, $\frac{3}{2}k\tilde{T} = E$, and $\gamma = 5/3$ (as for an ideal monatomic gas). We obtain $\tilde{p}V^{\gamma} = \frac{2}{3}EV^{2/3}$, and for a chaotic particle in a three-dimensional container, $\mu = \frac{4}{3}\pi(2mE)^{3/2}\, V \sim (EV^{2/3})^{3/2}$. Thus, constancy of $\tilde{p}V^{\gamma}$ again implies constancy of $\mu$.] See Appendix A for a discussion of the ergodic adiabatic invariant in relation to entropy and also for its implications for "quantum chaos."

The central question to be addressed in this paper is, How good is the ergodic adiabatic invariant? More specifically, what is the error incurred in the statement $\mu = \text{const}$? As we have already mentioned, in the case of $N = 1$ and periodic motion a quantity close to $\mu$ can be defined for which the error is smaller than any power of $\varepsilon$ for sufficiently smooth time variation of $H$. The case of the ergodic invariant with $N \geqslant 2$ has been considered theoretically by Ott,[11] using a multiple time scale expansion. His main result is an estimate of the typical rms error incurred by the approximation. (A precise statement of what is meant by the rms error is given in Section 3. For now we may think of it as a measure of the typical deviation of the squiggly surface in Fig. 1b from the smooth, constant-$H$ surface predicted by the ergodic adiabatic invariant.) The error estimate results in Ref. 11 depend on two hypotheses:

(a) The particle orbit in the frozen Hamiltonian is ergodic on the energy surface.

(b) A certain time correlation function $C(s)$ (to be defined later) for motion in the frozen Hamiltonian is integrable, $\int_0^{\infty} C(s)\, ds < \infty$, where $s$ denotes the time difference between the correlated quantities.

Thus, from (a), the derivation does not apply if motion in the frozen Hamiltonian has invariant tori (islands), while from (b), it does not apply

if, for example, the relevant correlation function has a long-time tail $C(s) \sim s^{-\xi}$ for $s \to \infty$ with $\xi \leqslant 1$.

The setting of Ref. 11 is that of Hamiltonians with smooth dependence on $\mathbf{p}$ and $\mathbf{q}$. However, we shall show that similar results apply for the case of chaotic billiard problems (Section 3). Combining the theoretical results of Ref. 11 with those to be derived in Section 3, we have the following:

1. If hypotheses (a) and (b) are satisfied, then the typical rms error in the ergodic adiabatic invariant is of order $\varepsilon^{1/2}$, and this applies both for smooth $(\mathbf{p}, \mathbf{q})$ variation (Ref. 11) and for billiards (Section 3).
2. If hypothesis (a) is satisfied, but (b) is violated with $C(s) \sim 1/s$ for large $s$, then the typical rms error is of order $[\varepsilon \ln(\varepsilon^{-1})]^{1/2}$.
3. If hypothesis (a) is satisfied, but (b) is violated with $C(s) \sim (1/s)^{\xi}$ $(0 < \xi < 1)$ for large $s$, then the typical rms error is of order $\varepsilon^{\xi/2}$.

Note, for example, that $C(s) \sim 1/s$ for the chaotic billiard example in Fig. 2. (This corresponds to case 2 above.) The existence of this type of long-time tail for a correlation function in the situation of Fig. 2 has been shown by Zacherl *et al.*[16] A modification of the billiard in Fig. 2 for which hypothesis (b) is satisfied[17] (case 1) is shown in Fig. 3.[8] Contrasting the theoretical results mentioned above {namely error scalings like $\varepsilon^{1/2}$,

[8] We do not know of an example where case 3 applies.

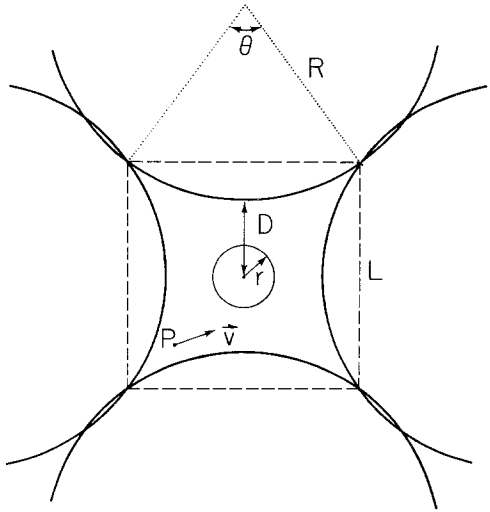


Fig. 3. Billiard with convex walls (Example 1).

$[\varepsilon \ln(\varepsilon^{-1})]^{1/2}$, and $\varepsilon^{\xi/2}$ with $0 < \xi < 1\}$ with the results for the case of periodic motion in $N = 1$ (where the error can be smaller than $\varepsilon^m$ for all finite $m$), we see that the adiabatic invariant approximation is in general not as good for the case of chaotic motion ($N \geqslant 2$) as for the case of periodic motion with $N = 1$.

The outline of the rest of this paper is as follows. Section 2 presents the results of computer experiments evaluating the rms error for three different slowly changing chaotic systems:

*Example 1.* The billiard in Fig. 3.

*Example 2.* The billiard in Fig. 2.

*Example 3.* The two-dimensional Hamiltonian given by

$$H(\mathbf{p}, \mathbf{q}; t) = (2m)^{-1}(p_x^2 + p_y^2) + gx^2 + y^2 + x^2y^2 \tag{3}$$

where $g = g(\varepsilon t)$ is a slow function of time to be specified later.

The results for the numerical experiments for Examples 1 and 2 are found to be in good agreement with theory. For Example 3, however, islands are present, and consequently there is no theory estimating the error in that case. Our numerical results for Example 3 show that the conservation of $\mu$ can still be a useful approximation if certain conditions are satisfied (in particular, the islands in the frozen Hamiltonian should not be too large). In Section 3 we review past theoretical work, consider the case $C(s) \sim s^{-\xi}$ ($\xi \leqslant 1$), and derive the previously mentioned theoretical results for the billiard case. Section 4 summarizes conclusions.

## 2. NUMERICAL RESULTS

In an effort to determine how well the ergodic adiabatic invariant $\mu$ is preserved, we have performed numerical experiments on the three dynamical systems (Examples 1–3) described in Section 1. The adiabatic invariant $\mu$ displays different distinct types of behavior for each of these systems. We believe that the behaviors displayed for these three examples are typical of what is to be expected for systems with the given characteristics. In particular, for Example 1, hypotheses (a) and (b) are satisfied; for Example 2, hypothesis (a) is satisfied, but (b) is not with $C(s) \sim 1/s$; and for Example 3, (a) is violated, but there is a connected "sea of chaos," which covers most of the energy surface (the islands are small). In this section we describe the experimental methods used to obtain and analyze our data and present the results of our numerical experiments.

### 2.1. Example 1

The billiard we call Example 1 represents a best case scenario in the sense that neither hypothesis (a) nor hypothesis (b) is violated. For all billiards, we have that

$$\mu = 2\pi mEA \tag{4}$$

where $E$ is the energy of the system and $A$ is the area of the confining region. [This follows since the configuration space area available to a particle of energy less than $E = p^2/2m$ is clearly just $A$ (independent of $E$), while the available momentum space area is $\pi p^2 = 2\pi mE$.] The area of the confining region for Example 1 is

$$A = L^2 - \pi r^2 - 2R^2(\theta - \sin\theta) \tag{5}$$

where $r$, $L$, $R$, and $\theta$ are shown in Fig. 3.

The theoretical results in both Ref. 11 and Section 3 are statistical in nature. They predict the behavior of the variance of $\mu$ about its mean value. In order to test these predictions, our numerical experiments used an ensemble of $M \gg 1$ different initial conditions $(\mathbf{p}(0), \mathbf{q}(0))$, uniformly distributed over an $H(\mathbf{p}, \mathbf{q}; 0) = \text{const}$ phase space hypersurface. For billiards $H = \mathbf{p} \cdot \mathbf{p}/2m + V(\mathbf{q}; t)$, where the potential $V$ acts only at the walls of the box. Thus, inside the confining region, $H$ is only a function of the magnitude of $\mathbf{p}$. Therefore, the $\mathbf{q}(0)$'s were selected at random inside the confining region, while the $\mathbf{p}(0)$'s were given unit magnitude and random orientation. For convenience the mass of the particle was fixed at $m = 1$.

For all billiards, a "slow" time dependence can be added to the system by slowly changing the size and shape of the confining region. Let $\mathbf{w}$ be the velocity of the moving wall of the confining region at the point where the particle strikes the wall ($\mathbf{w}$ is taken to be normal to the wall). If $\mathbf{w} \cdot \mathbf{p} > 0$, the particle will lose energy as it is specularly reflected. Conversely, if $\mathbf{w} \cdot \mathbf{p} < 0$, the particle will gain energy. However, $\mu$ will remain adiabatically invariant. In Example 1 we oscillate the large circles according to the rule $D = D_0 - \Delta D \cos(2\pi t/T)$, where $D$ is the distance shown in Fig. 3. The radius $r$ of the central circle as well as the radius of curvature $R$ of the convex walls are held fixed in time. Thus, change of $D$ is accomplished by moving the centers of curvature of the convex walls in and out (refer to Fig. 3). The "slowness" of the time dependence is controlled by the parameter $T$. The $T$ values we used in our numerical experiments ranged from a minimum of 100 to a maximum of 10,000. By oscillating $D$, the quantities $L$ and $\theta$ shown in Fig. 3 will be time-dependent. Explicit expressions for $L$ and $\theta$ as a function of $D$ are $L = R + D - (R^2 - D^2 - 2RD)^{1/2}$ and $\theta = 2\sin^{-1}(L/2R)$.

There are geometrical constraints on the possible values that we can assign to $D_0$, $\Delta D$, $R$, and $r$. An examination of Fig. 3 indicates the nature of these constraints. In particular, we do not want the large circles to intersect the small circle during the oscillation. Similarly, we do not want the large circles to become disjoint from each other during the oscillation. The latter constraint ensures that the particle is permanently trapped. For the model in Fig. 3 these constraints are $(\sqrt{2}-1)R \geqslant D > r$. For our numerical experiments we used the following parameter values: $r=1$, $D_0=2$, $\Delta D=0.5$, and $R=6.297\ldots$.

Our numerical experiments for Example 1 proceed as follows. We evolve each of the $M$ randomly chosen initial conditions with time. Between reflections the particles move with constant velocity $\mathbf{v}$. At reflections from a moving wall we change the particle's velocity from $\mathbf{v}_-$, before hitting the wall to $\mathbf{v}_+$ after hitting the wall, via

$$\mathbf{v}_+ = \mathbf{v}_- + 2[\mathbf{w} - (\hat{\mathbf{n}} \cdot \mathbf{v}_-)\hat{\mathbf{n}}]$$

where $\hat{\mathbf{n}}$ is the unit normal to the wall (taken outward from the accessible area) at the impact point, and $\mathbf{w}$ is the local normal wall velocity. This reflection law is obtained by noting that, in the frame moving with the local wall velocity, the reflection is as for a stationary planar wall (i.e., in this frame the angle of incidence equals the angle of reflection and energy is conserved). At any given time, each particle has an energy $E_i(t)$, where $i$ labels the particle ($i=1, 2,\ldots, M$). We then calculate the quantity

$$\mu_i(t) = E_i(t)\, A(t)$$

for each particle. Averages

$$\delta(t) \equiv \frac{1}{M} \sum_{i=1}^{M} (\mu_i(t) - \mu_0) = \bar{\mu} - \mu_0$$

$$\sigma^2(t) \equiv \frac{1}{M} \sum_{i=1}^{M} [\mu_i(t) - \bar{\mu}]^2$$

are then calculated, where $\mu_0$ is the initial value of all the $\mu_i(t)$ $[\mu_i(0) \equiv \mu_0]$ and $\bar{\mu}$ is their mean value.

We calculate $\delta$ and $\sigma^2$ at $t=T/2$ as well as at $t=T$ for a range of $T$ values and investigate their dependence on the slowness $T$. We also examined the behavior of $\sigma^2$ as the system proceeds through many oscillations of the fundamental period $T$.

The results of our numerical experiments on Example 1 are shown in Fig. 4. In all of the figures the straight lines are least square error lines of

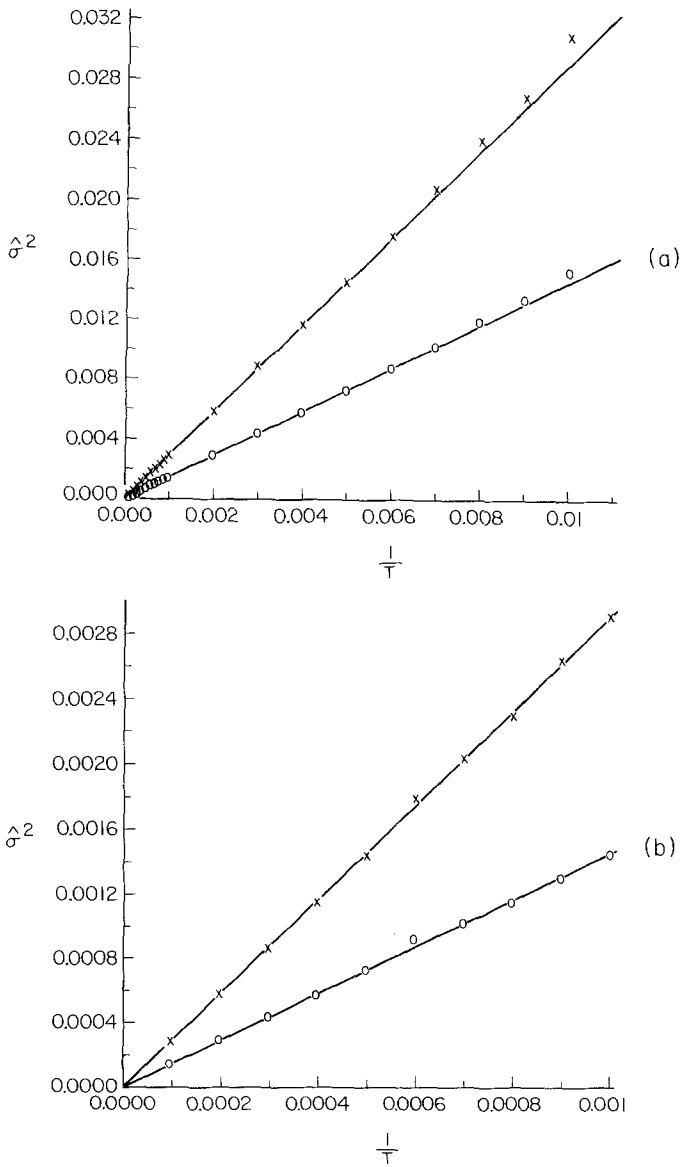


Fig. 4. (a) Results of numerical experiments on a billiard with convex walls (Example 1). The results shown are for $T \in [100, 10000]$ and an ensemble average of 50,000 particles. Data taken at ($\times$) $t = T$ and ($\circ$) $t = T/2$. Notice that the error in the adiabatic invariant scales like $\varepsilon^{1/2}$. (b) The same as (a), except for $T \geqslant 1000$. (c) The drift of the adiabatic invariant at time $t = T$ away from its initial value. Notice the linear dependence of $\delta$ on $\varepsilon$. Comparison with (a) indicates that $\delta/\hat{\sigma} \sim \sqrt{\varepsilon} \ll 1$ in the $T \to \infty$ limit. (d) Same as (c), except for $t = T/2$. (e) The ratio of $\sigma^2(nT)/\sigma^2(T)$ versus $n$. The linear relationship indicates the diffusive nature of $\sigma^2(t)$.

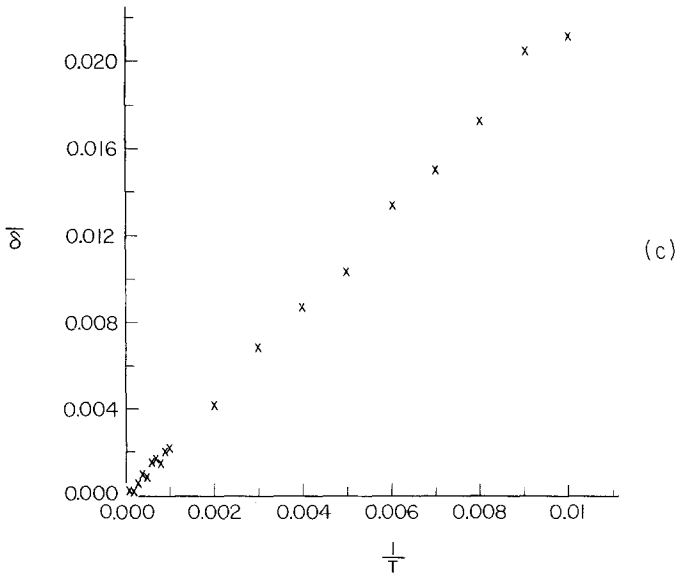


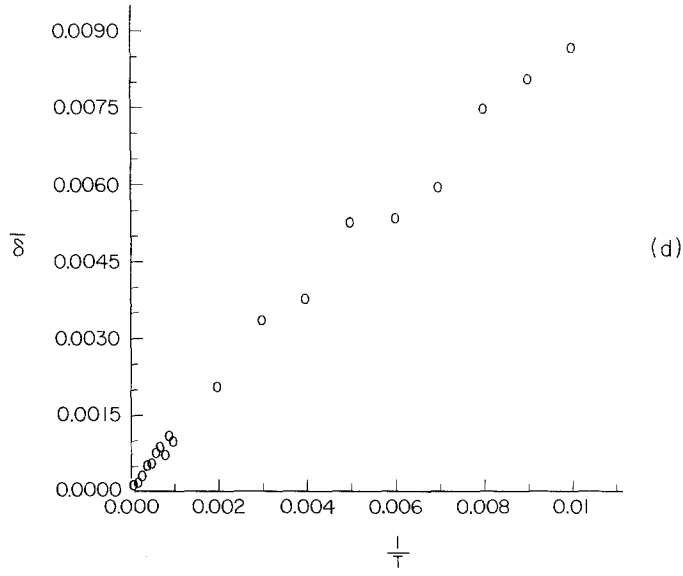


Fig. 4 (*continued*)

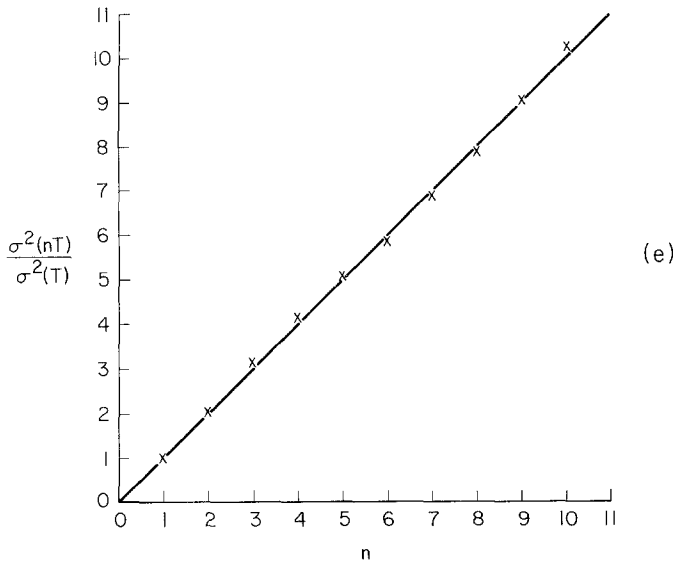


Fig. 4 (*continued*)

best fit for the data (for Fig. 4a only the $T \geqslant 1000$ data are used for the fit). The data indicated by crosses and circles in Fig. 4 correspond to $\sigma^2$ and $\delta$ evaluated at $t = T$ and $t = T/2$, respectively. In Figs. 4a and 4b the abscissa is the slowness parameter $\varepsilon \equiv 1/T$ and the ordinate is $\hat{\sigma}^2 \equiv \sigma^2/(\mu_0)^2$, the normalized variance of $\mu$ about its mean. In these figures we used an ensemble of $M = 50{,}000$ particles. As one can see from Figs. 4a and 4b, the expected linear relationship between $\sigma^2$ and $\varepsilon$ is found throughout almost the entire range of $\varepsilon$. In Fig. 4b we plot some of the same data as in Fig. 4a but only for $T \geqslant 1000$. A close examination of the data for $M = 50{,}000$ reveals that it exhibits an extremely small amount of scatter about the line of best fit. (On the scales shown in Figs. 4a and 4b the scatter is too small to be seen.) We have measured $\varsigma$, the standard deviation of this scatter, for ensembles of size $M_1 = 100$ and $M_2 = 5000$. In both cases it was found that the ratio of the standard deviations from the line of best fit scaled like $\varsigma(M)/\varsigma(M_i) \simeq (M_i/M)^{1/2}$ for $i = 1, 2$, in agreement with the scaling predicted by probability theory. Therefore, we believe this scatter is statistical in nature.

Figures 4c and 4d show plots of $\bar{\delta} \equiv \delta/\mu_0$ versus $1/T$ ($M = 50{,}000$). In agreement with the theoretical results of Section 3, we see that the data are well fit by a linear dependence of $\delta$ on $1/T$, $\delta \sim 1/T$. Since $\hat{\sigma}^2 \sim 1/T$, we see that $\bar{\delta}/\hat{\sigma} \sim 1/\sqrt{T} \ll 1$. Thus, the error incurred in predictions based on the constancy of the ergodic adiabatic invariant $\mu$ is primarily due to $\hat{\sigma}^2$, the variance about the mean value of $\mu$, rather than $\delta$, the drift of the mean

value away from the initial value $\mu_0$. We found similar results for Examples 2 and 3. Therefore, for Examples 2 and 3 we will only show plots indicating the behavior of $\hat{\sigma}^2$ rather than $\bar{\delta}$, since $\hat{\sigma} \gg \bar{\delta}$ in the adiabatic limit.

Having established that the principal source of error in the adiabatic invariant is given by $\hat{\sigma}^2$, we return to Fig. 4a. From this figure we see that the relative error $\hat{\sigma}$ in the adiabatic invariant (measured at $t = T$) is less than 10% for $T > 300$ and less than 1% for $T > 30{,}000$. We are also interested in the relative error in the energy predicted by the adiabatic invariant. Thus, we define a relative energy error $\eta_E$ by

$$\eta_E \equiv \langle (\Delta H)^2 \rangle^{1/2} / |\bar{E}(T/2) - E(0)| \tag{6}$$

where $E(0) \equiv 1/2$ and $\bar{E}(t)$ is the particle energy predicted by the conservation of the adiabatic invariant [Eq. (1)], and

$$\langle (\Delta H)^2 \rangle \equiv \frac{1}{M} \sum_{i=1}^{M} [E_i - \bar{E}(t)]^2$$

is evaluated at $t = T/2$. [Note that $\langle (\Delta H)^2 \rangle \simeq \sigma^2 / (\partial \mu / \partial E)^2$.] The numerical values of the relative energy error $\eta_E$ corresponding to the $T$ ranges above are less than 3% for $T > 300$ and 0.3% for $T > 30{,}000$.

In Fig. 4e we plot the ratio $\sigma^2(nT)/\sigma^2(T)$ versus $n$, the number of oscillations ($M = 5000$). The linear relationship shown in Fig. 4e indicates that the evolution of $\sigma^2$ over multiple oscillation times is diffusive (i.e., the variance after $n$ oscillations of period $T$ is approximately the product of the variance for a single oscillation of period $T$ and $n$, the number of times the system oscillates).

## 2.2. Example 2

We now turn out attention to Example 2. This system is also a billiard, and is shown in Fig. 2. Example 2 illustrates one possible configuration where hypothesis (a) is satisfied, but hypothesis (b) is violated. Specifically, $C(s) \sim 1/s$ for large $s$. Since this system is also a billiard, the ergodic adiabatic invariant is given by Eq. (4), with $A = L^2 - \pi r^2$.

The existence of a long-time $1/s$ tail in the correlation function for the (time-independent) billiard in Fig. 2 has been demonstrated by Zacherl *et al.*[16] This long-time tail arises due to particles that bounce between parallel walls for many bounces, as illustrated in Fig. 5. A particle that makes $\hat{t}$ bounces or more with the parallel walls before colliding with

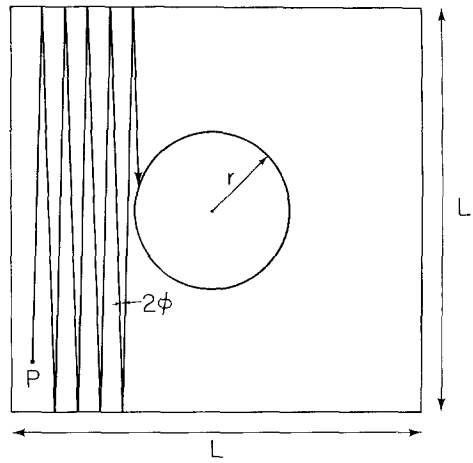


Fig. 5. For small $\phi$ the particle bounces many times before colliding with the circle. Such trajectories can mimic a periodic orbit (exactly vertical or exactly horizontal) for very long times.

the central circular boundary is traveling nearly vertically (or horizontally), and its velocity makes an angle $\phi$ to the vertical that must be small enough,

$$\phi < O(1/\hat{t})$$

At any given time let $\hat{f}$ denote the fraction of particles that subsequently make at least $\hat{t}$ such bounces. Then, due to the ergodicity[15] of the particle motion in the billiard,

$$\hat{f} \sim 1/\hat{t}$$

This relatively large number of particles behaving in a coherent, close to periodic manner for $\hat{t}$ or more bounces is what leads to the long-time $1/s$ tail. Put another way, the periodic orbit represented by a particle moving exactly in the vertical (or equivalently horizontal) direction (and not hitting the circle) has neutral stability. The family of such periodic orbits has zero measure in phase space, but, as a result of its neutral stability, a relatively large measure of the particles mimic it for a *finite* time (i.e., $\hat{f} \sim 1/\hat{t}$). In contrast, for the billiard of Fig. 3 all periodic orbits are *exponentially* unstable. Thus, the fraction of particles that mimic a periodic orbit for the Fig. 3 billiard for $\hat{t}$ or more bounces is exponentially small in $\hat{t}$, and a long-time tail is absent. We emphasize that the above arguments are only meant as a guide to intuition and refer the interested reader to Refs. 16 and 17, where the cases of the billiards of Figs. 2 and 3 are treated more rigorously.

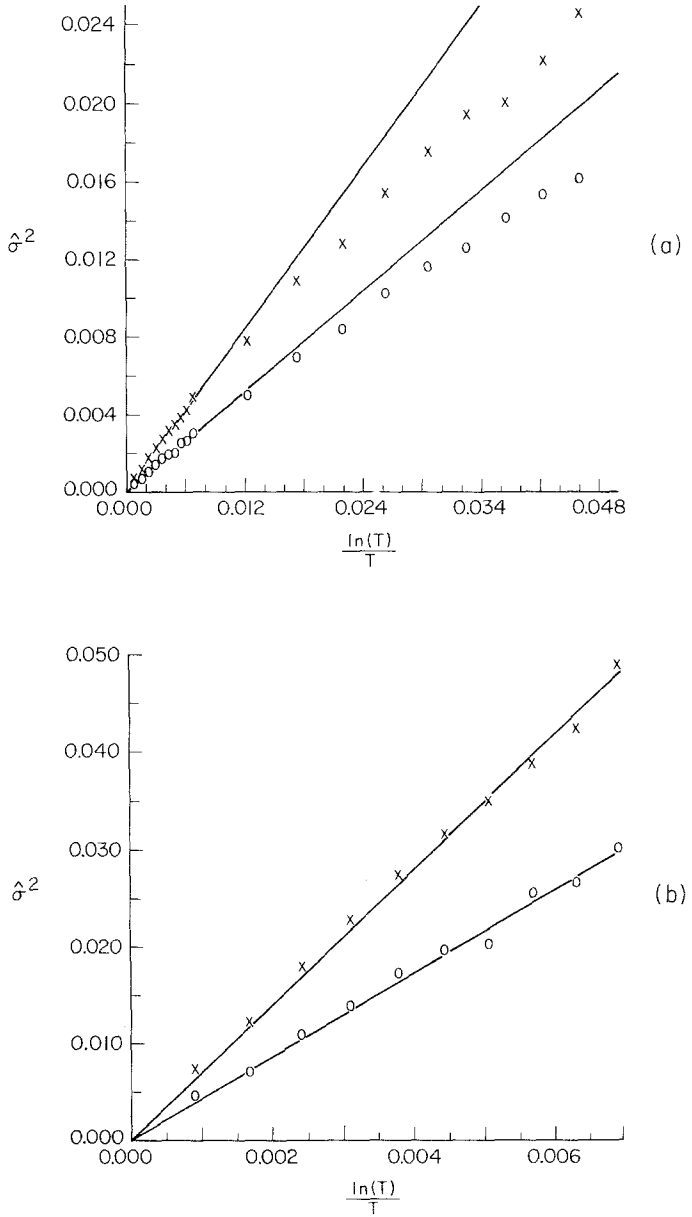


Fig. 6. (a) Results of numerical experiments on the square billiard (Example 2). The results shown are for $T \in [100, 10000]$ and an ensemble average of 5000 particles. Data taken at ($\times$) $t = T$ and ($\circ$) $t = T/2$. Notice that the error in the adiabatic invariant scales like $[\varepsilon \ln(\varepsilon^{-1})]^{1/2}$ in the $T \to \infty$ limit. (b) Same as (a), except for $T \geqslant 1000$. (c) Ratio of $\sigma^2(nT)/\sigma^2(T)$ versus $n$. The linear relationship indicates that this billiard is also diffusive.

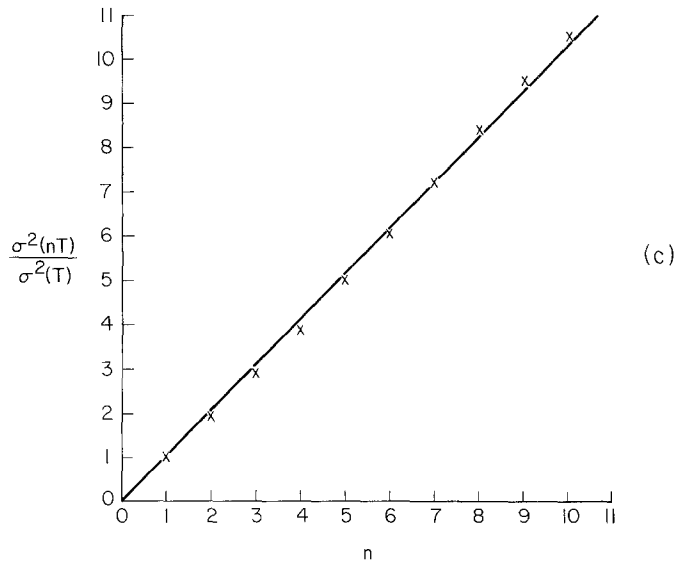


Fig. 6 (*continued*)

The ensemble of $M = 5000$ initial conditions we employ in Example 2 is chosen in the same manner as those in Example 1. Similarly, we add an explicit time dependence to the system by oscillating $L$, the length of the walls of the confining region, via the rule $L/2 = L_0 - \Delta L \cos(2\pi t/T)$; $r$ is kept fixed in time. In our numerical experiments $T$ ranged from a minimum of 100 to a maximum of 10,000. The only geometrical constraint on this billiard is $L_0 - \Delta L > r$. We chose parameter values of $L_0 = 2$, $\Delta L = 0.5$, $r = 1$, $m = 1$, and initial speed one.

The results of our numerical experiments on Example 2 are shown in Fig. 6. In Figs. 6a and 6b the abscissa is $\varepsilon \ln(\varepsilon^{-1}) \equiv (\ln T)/T$ and the ordinate is $\hat{\sigma}^2 \equiv \sigma^2/(\mu_0)^2$, the normalized variance of $\mu$ about its mean. In Figs. 6a and 6b the crosses denote data taken at $t = T$ and the circles denote data taken at $t = T/2$. The straight lines are least square error lines of best fit using the data in the asymptotic region ($T \geqslant 1000$). We expect (cf. Section 3) that $\hat{\sigma}^2$ will depend linearly on $(\ln T)/T$. Figure 6a shows that for the range of $T$ values used, $\hat{\sigma}^2$ asymptotes to a linear dependence on $(\ln T)/T$ for large $T$. This behavior is further confirmed in Fig. 6b, which plots the same two variables, but only for $T \geqslant 1000$. Within this range of $T$ values the dependence of $\hat{\sigma}^2$ is extremely well fit by its predicted linear dependence on $(\ln T)/T$. From Figs. 6a and 6b we see that the relative error $\hat{\sigma}$ in the adiabatic invariant (measured at $t = T$) is less than 10% for $T > 400$ and less than 1% for $T > 75{,}000$. The relative energy error $\eta_E$

[Eq. (6)] corresponding to the $T$ ranges above are 4% for $T > 400$ and 0.4% for $T > 75{,}000$.

Note that, in comparison with Example 1, much larger $T$ values are required before $\hat{\sigma}^2$ is accurately fit by its asymptotically predicted behavior. That is, for Figs. 4a and 4b the straight line fit is good for $T \geqslant 200$, while for Figs. 6a and 6b, $T \geqslant 1000$ is required. This is not unexpected, since, due to the predicted forms of the error in the two cases, we might guess that the conditions for the asymptotic regimes to apply are $T \gg 1$ for Example 1 and $\ln T \gg 1$ for Example 2.

In Fig. 6c we plot the ratio $\sigma^2(nT)/\sigma^2(T)$ versus $n$, where $T = 1000$ and $n$ is the number of oscillation times of the system. The behavior of the present example is qualitatively the same as that of Example 1. Hence, for this billiard the evolution of $\sigma^2$ over multiple oscillations of the system geometry is also diffusive.

## 2.3. Example 3

For our last example we examine a dynamical system where hypothesis (a) is violated. We consider the following Hamiltonian:

$$H(\mathbf{p}, \mathbf{q}; \varepsilon t) \equiv (2m)^{-1}(p_x^2 + p_y^2) + g(t)x^2 + y^2 + x^2y^2 \tag{7}$$

where $g(t) = [7 - \cos(2\pi t/T)]/6$. Unlike billiards, the phase space trajectories are continuous. The equations of motions for particle trajectories are given by Hamilton's equations.

In Appendix B we perform the integral given by Eq. (1) for the Hamiltonian given by Eq. (7). The result of this calculation is

$$\mu(E, t) = \frac{16\pi m(g+E)^{1/2}}{9}\left[(3E+2g)\,F(k) - (4E+2g)\,K(k)\right] \tag{8}$$

where $k^2 \equiv E/(g+E)$, $E$ is the energy of the system, and $F(k)$ and $K(k)$ are complete elliptic integrals of the first and second kind, respectively.

In our numerical experiments we considered $m = 1$ and an initial energy of $E = 24$. Figure 7 shows surface-of-section plots for the time-independent Hamiltonian system obtained by freezing $t$ in Eq. (7) at $t = 0$, $T/8$, $T/4$, $3T/8$, and $T/2$ and using the corresponding energies obtained from the prediction of the adiabatic invariant,

$$\mu(E(t), t) = \mu(24, 0)$$

at $t = 0$, $T/8$, $T/4$, $3T/8$, and $T/2$. The surface of section is obtained by plotting $y(t)$ and $p_y(t)$ every time an orbit crosses the plane $x = 0$ with

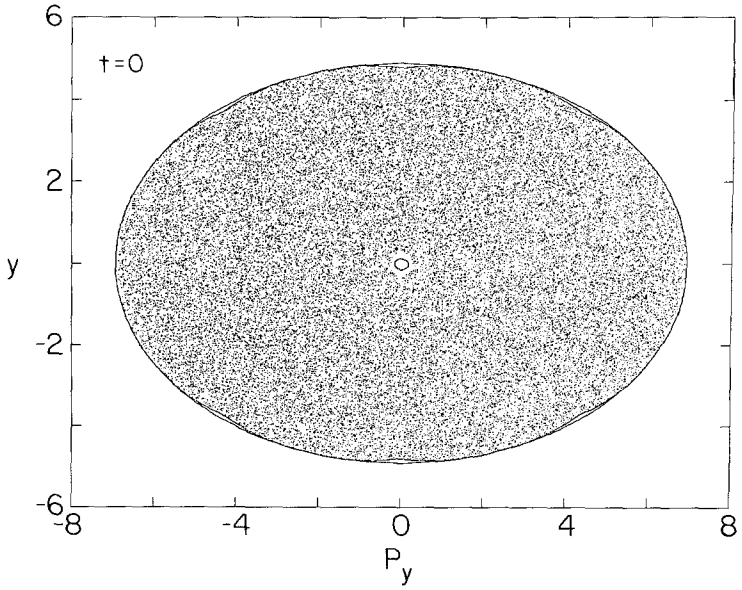


(a)

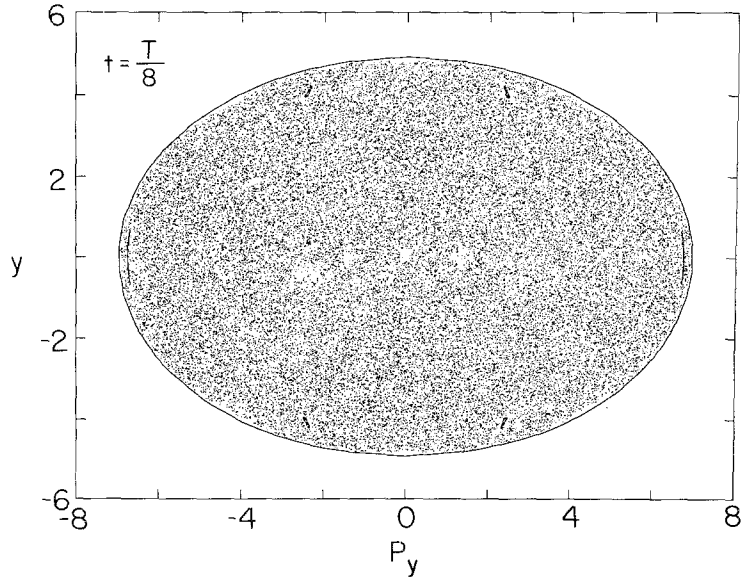


(b)

Fig. 7. Typical surface of sections for the frozen Hamiltonian at $H=24$ and $t=$ (a) 0, (b) $T/8$, (c) $T/4$, (d) $3T/8$, and (e) $T/2$.

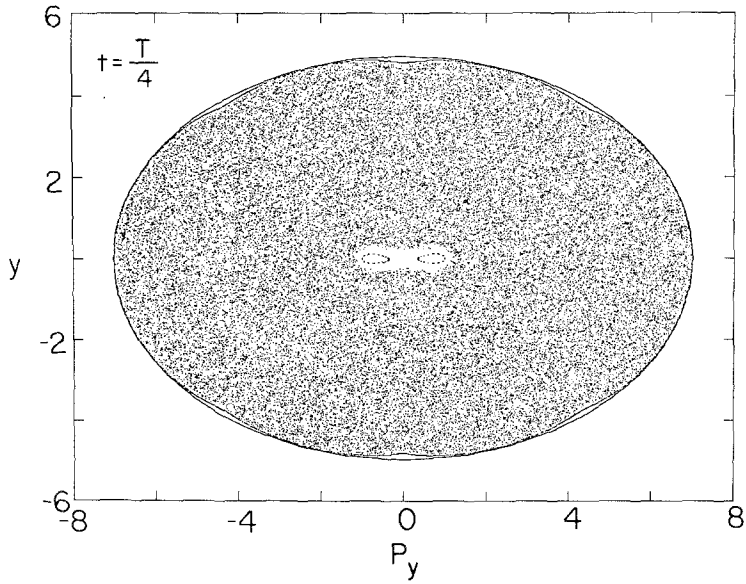


(c)

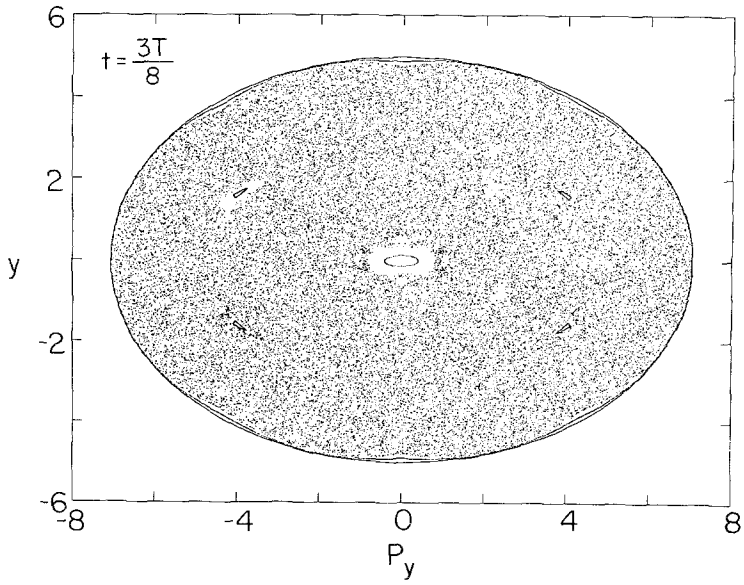


(d)

Fig. 7 (*continued*)

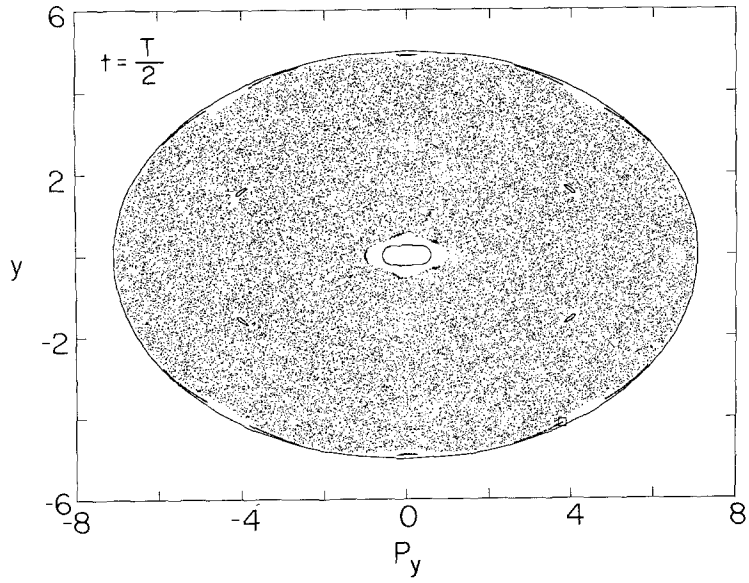


(e)

Fig. 7 (*continued*)

$p_x > 0$. For $x = 0$, $H = (2m)^{-1}(p_x^2 + p_y^2) + y^2$, and thus all points in the surface of section fall within the area defined by $E \geqslant y^2 + p_y^2/2m$. In each of the surface-of-section plots several choices of initial conditions are superposed. In all cases, however, most of the area shown is filled by a single chaotic orbit generated from one initial condition. Other initial conditions that trace out smooth closed curves (tori) are also evident. These, however, are seen to enclose only a small fraction of the available $y$–$p_y$ area. Thus, although hypothesis (a) is violated, typical particles still sample *most* of the energy surface. Hence, we might expect the adiabatic invariant to still provide a useful approximation, and this is what we wish to test. Our hope is that these numerical results will be typical of what happens in other situations where tori are present but only occupy a small fraction of the energy surface.

A word is in order about our choice of potential in Eq. (7), namely, $V = g(t)x^2 + y^2 + x^2y^2$. We wanted to have a Hamiltonian where the area occupied by islands was not large and could be decreased by increasing the energy. Thus, a reasonable place to start is with a potential that has no islands at all (i.e., a completely chaotic case). Such a case is the potential[18] $V = x^2y^2$. Note, however, that this potential is unsuitable for testing the adiabatic invariant, since the integral for $\mu$ [Eq. (1)] is infinite. Thus, we

have added the confining quadratic terms $g(t)x^2 + y^2$, which prevent particles from running off to large $x$ along $y \simeq 0$ and large $y$ along $x \simeq 0$ and hence restores a finite value to $\mu$. Our choice of the time dependence as occurring only multiplying the $x^2$ term was somewhat arbitrary, but satisfied our desire to make the time dependence asymmetric in $x$ and $y$; e.g., we wanted to avoid the choice $g(t)(x^2 + y^2) + x^2y^2$.

For the numerical experiments we used $M = 12{,}800$ particles and, at $t = 0$, randomly distributed them uniformly over the $H = 24$ energy surface. The initial distribution we wish to simulate can be written as $F(\mathbf{p}, \mathbf{q}; 0) = K\delta[E - H(\mathbf{p}, \mathbf{q}; 0)]$, where $K$ is a constant such that $\int d^2p\, d^2q\, F(\mathbf{p}, \mathbf{q}; 0) = 1$. The corresponding configuration space density is $\rho(\mathbf{q}) = \int F(\mathbf{p}, \mathbf{q}; 0)\, d^2p$. Since $H = \mathbf{p} \cdot \mathbf{p}/2m + V(\mathbf{q})$, we have $\rho(\mathbf{q}) = 2\pi KmU[E - V(\mathbf{q})]$; i.e., the distribution in position space is uniform in the allowed region. Thus, to generate a suitable initial ensemble numerically we first choose an ensemble of position coordinates uniform in $E \geqslant V(\mathbf{q})$. This is accomplished by randomly choosing $x$, $y$ coordinates uniform in $|x| \leqslant \sqrt{E}$ and $|y| \leqslant \sqrt{E}$ [recall that $g(0) = 1$]. We calculate $V(\mathbf{q})$ for each such point. If $V(\mathbf{q}) > E$, the point is rejected. If $V(\mathbf{q}) \leqslant E$, the point is kept. We then specify the momentum to have magnitude $|\mathbf{p}| = \{2m[E - V(\mathbf{q})]\}^{1/2}$, randomly choose $\theta \in (0, 2\pi]$, and then set $p_x = |\mathbf{p}| \cos\theta$, $p_y = |\mathbf{p}| \sin\theta$. Applying this recipe for point selection, we generate an ensemble of initial points that simulates a uniform distribution over the $H = 24$ energy surface.

The results of our numerical experiments on Example 3 are shown in Fig. 8. Figure 8a is a log–log plot of $\hat{\sigma}^2 \equiv \sigma^2/(\mu_0)^2$ versus $\varepsilon \equiv 1/T$. For large values of $T$ the data asymptotes to a straight line. This linear relationship indicates that in the adiabatic limit, $\hat{\sigma}^2 \sim (1/T)^{\xi}$, where $\xi$ is the slope of the line in Fig. 8a. In Fig. 8b we plot the same variables, but only for $T \geqslant 1000$. Once again the crosses and circles represent data taken at $t = T$ and $t = T/2$, respectively, while the straight lines are least square error lines of best fit using only the data for $T \geqslant 3000$.

From Fig. 8b, we see that the data at $t = T$ are rather well fit by the fitted straight line, which has a slope of $\xi \simeq 0.41$. The data for $t = T/2$, however, have a good deal more scatter and the fitted slope is correspondingly not as reliable, $\xi \simeq 0.24$. While the two values of $\xi$ at $T$ and $T/2$ differ and the results have a good deal of scatter, the general trend for the error $\hat{\sigma}^2$ to decrease with increasing $T$ is apparent. We caution, however, that no theory is available for this case, and consequently care must be taken in interpreting these results. In particular, although the fit to a power law is fairly good for the $t = T$ data in Fig. 8b, we cannot be certain that a similarly good fit would persist as $T$ is made larger (computer time limitations prevent us from extending our data in this direction). From Figs. 8a and 8b we see that when we extrapolate $T$ to the range $T > 40{,}000$

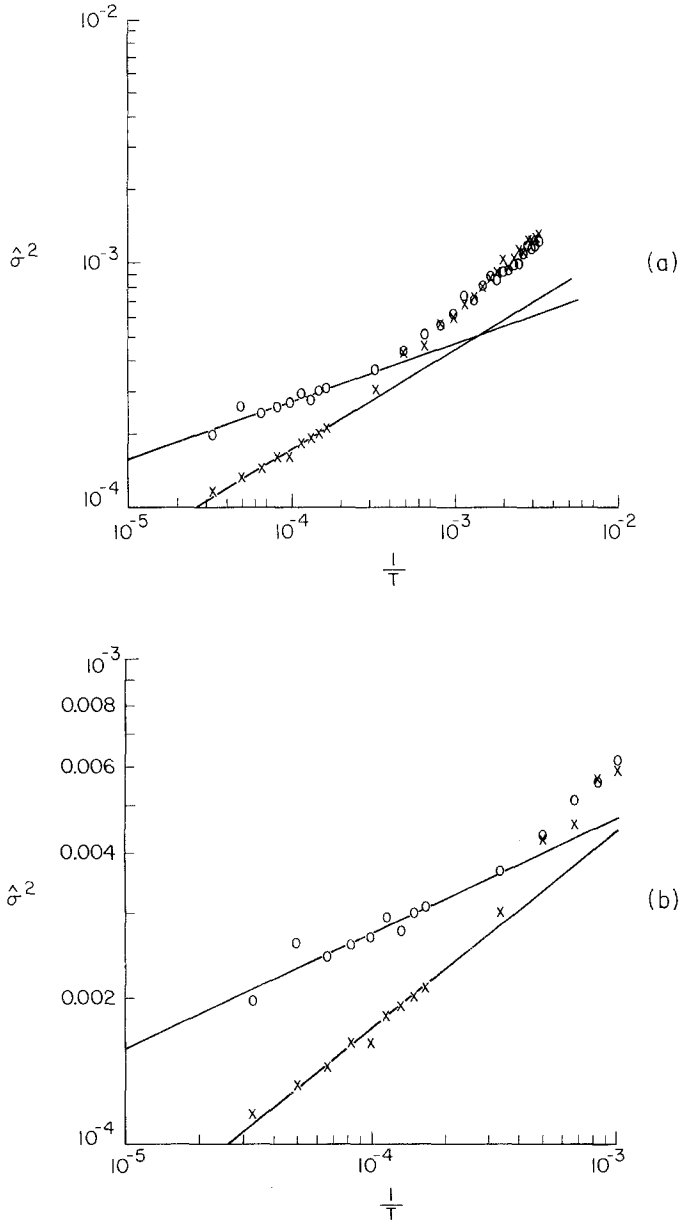


Fig. 8. (a) Results of numerical experiments on the Hamiltonian of Example 3. The results shown are for $T \in [300, 30000]$ and an ensemble of 12,800 particles. Data taken at ( $\times$ ) $t = T$ and ( $\bigcirc$ ) $t = T/2$. (b) Same as (a), except for $T \geqslant 1000$. (c) The ratio of $\sigma^2(nT)/\sigma^2(T)$ versus $n$. The linear relationship between these two variables indicates that the Hamiltonian is also diffusive.

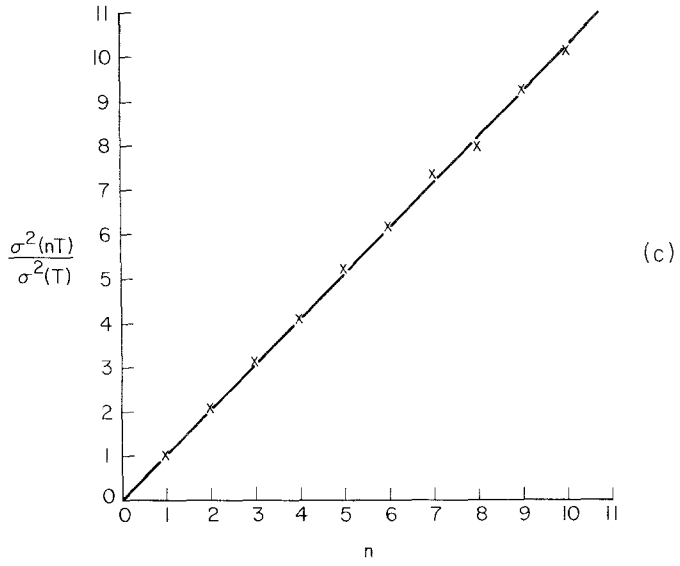


Fig. 8 (*continued*)

the relative error $\hat{\sigma}$ in the adiabatic invariant is less than 1%. We also find that the relative energy error $\eta_E$ [Eq. (6)] is less than 12% for $T > 40{,}000$. Comparing the results of Example 3 with those of Examples 1 and 2, we see that the scaling of the error in the adiabatic invariant is worse for Example 3, as expected.

In Fig. 8c we plot $\sigma^2(nT)/\sigma^2(T)$ versus $n$, the number of oscillations ($T = 6000$). The linear relationship between these two quantities is again indicative of the diffusive nature of $\sigma^2$.

## 3. THEORETICAL CONSIDERATIONS

In this section we provide a theoretical basis for the numerical results we reported in Section 2. We begin by discussing Hamiltonians that depend smoothly on **p**, **q**, and $t$, that is, $H$ is assumed to be differentiable in these variables. After this type of system has been analyzed, we will consider billiards. Let $E(t)$ denote the value of the energy at time $t$ predicted by the conservation of $\mu$ [i.e., $\mu(E(t), t) = \mu(E(0), 0)$]. Consider a particle in the ensemble initially on the energy surface $H(\mathbf{p}, \mathbf{q}; 0) = E(0)$. At some latter time this particle will have an energy slightly different from the predicted value. That is, for this particle $H \neq E(t)$. If we expand $\mu$ in a Taylor series about $E$, we have

$$\Delta\mu = \frac{\partial\mu(E)}{\partial E}\Delta H + \frac{1}{2}\frac{\partial^2\mu(E)}{\partial E^2}(\Delta H)^2 + O((\Delta H)^3) \tag{9}$$

where $\Delta\mu \equiv \mu(H) - \mu(E)$ and $\Delta H \equiv H - E$. Furthermore,

$$(\Delta\mu)^2 = \left(\frac{\partial\mu(E)}{\partial E}\right)^2 (\Delta H)^2 + \frac{\partial\mu(E)}{\partial E}\left(\frac{\partial^2\mu(E)}{\partial E^2}\right)(\Delta H)^3 + O((\Delta H)^4) \quad (10)$$

If we then take the ensemble average of $\Delta\mu$ and $(\Delta\mu)^2$, we have

$$\langle\Delta\mu\rangle \simeq \frac{\partial\mu(E)}{\partial E}\langle\Delta H\rangle + \frac{1}{2}\frac{\partial^2\mu(E)}{\partial E^2}\langle(\Delta H)^2\rangle \quad (11)$$

$$\langle(\Delta\mu)^2\rangle \simeq \left(\frac{\partial\mu(E)}{\partial E}\right)^2 \langle(\Delta H)^2\rangle \quad (12)$$

As we shall show, $\langle\Delta H\rangle$ and $\langle(\Delta H)^2\rangle$ are of the same order, while the contributions from the terms $\langle O((\Delta H)^3)\rangle$ are of higher order in $T^{-1}$; thus, these terms have been omitted in Eqs. (11) and (12). We now calculate $\langle(\Delta H)^2\rangle$ and $\langle\Delta H\rangle$, from which $\langle(\Delta\mu)^2\rangle$ and $\langle\Delta\mu\rangle$ are determined by Eqs. (11) and (12).

### 3.1. Analysis for Smooth Hamiltonian Systems

Consider an ensemble of initial conditions uniform on an energy hypersurface $H(\mathbf{p}, \mathbf{q}; 0) = E(0)$, where $\mathbf{p}$ and $\mathbf{q}$ are $N$-vectors. The distribution function for such an ensemble can be written as

$$F(\mathbf{p}, \mathbf{q}; 0) = K(0)\,\delta[H(\mathbf{p}, \mathbf{q}; 0) - E(0)] \quad (13)$$

where $F$ is normalized so that $\int F\,d^N p\,d^N q = 1$ [this determines $K(0)$]. The time evolution of this initial distribution function is governed by the Liouville equation,

$$\frac{\partial F}{\partial t} + \frac{\partial H}{\partial \mathbf{p}}\cdot\frac{\partial F}{\partial \mathbf{q}} - \frac{\partial H}{\partial \mathbf{q}}\cdot\frac{\partial F}{\partial \mathbf{p}} = 0 \quad (14)$$

As our ensemble of initial conditions evolves in time, a given realization in the ensemble will in general gain or lose slightly more or less energy than that predicted by the adiabatic invariant. We then ask, what is the time dependence of the first and second moments of the deviation of the energy from the energy value obtained from $\mu = \text{const}$? The second moment $\langle(\Delta H)^2\rangle$ represents the spread of the energies in the ensemble about the value $E(t)$, while the first moment $\langle\Delta H\rangle$ represents the drift of the mean energy of the ensemble away from $E(t)$. We first show how to obtain the time evolution of the second moment. (We shall return to the first moment subsequently.) An equation that gives the time dependence of the second

moment can be derived by multiplying Eq. (14) by $(H-E)^2$ and integrating over phase space. After an integration by parts, we have

$$\frac{d}{dt}\langle(\Delta H)^2\rangle = 2\int F(H-E)\left(\frac{\partial H}{\partial t}-\frac{dE}{dt}\right)d^N p\, d^N q \tag{15}$$

where

$$\langle(\Delta H)^2\rangle \equiv \int (H-E)^2 F\, d^N p\, d^N q$$

The problem then becomes that of obtaining a sufficiently good approximation to $F$ to insert into Eq. (15) so as to obtain a nontrivial approximation to $d\langle(\Delta H)^2\rangle/dt$. To do this, Ott[11] has applied a two-time-scale asymptotic technique to solve the Liouville equation (14) subject to the initial condition (13). He assumed that $F$ could be written as a part $F_0$ that changed on the slow time scale defined in Section 1 plus a small correction term that depended on both the fast and slow time scales, as well as higher order terms. Thus,

$$H(\mathbf{p}, \mathbf{q}; t) = h(\mathbf{p}, \mathbf{q}; \tau_2) \tag{16}$$

$$F(\mathbf{p}, \mathbf{q}; t) = F_0(\mathbf{p}, \mathbf{q}; \tau_2) + \varepsilon F_1(\mathbf{p}, \mathbf{q}; \tau_1, \tau_2) + O(\varepsilon^2) \tag{17}$$

$$\tau_1 = t, \qquad \tau_2 = \varepsilon t, \qquad \varepsilon \ll 1 \tag{18}$$

where $\varepsilon$ is defined in Section 1. The fast and slow time variables $\tau_1$ and $\tau_2$ are treated as independent variables. As such, the time derivative in Eq. (14) becomes $\partial/\partial t = \partial/\partial\tau_1 + \varepsilon\,\partial/\partial\tau_2 + O(\varepsilon^2)$. By using this and inserting Eqs. (16)–(18) into Eq. (14), we obtain

$$\frac{\partial h}{\partial \mathbf{p}}\cdot\frac{\partial F_0}{\partial \mathbf{q}} - \frac{\partial h}{\partial \mathbf{q}}\cdot\frac{\partial F_0}{\partial \mathbf{p}} = 0 \tag{19}$$

$$\frac{dF_1}{d\tau_1} \equiv \frac{\partial F_1}{\partial \tau_1} + \frac{\partial h}{\partial \mathbf{p}}\cdot\frac{\partial F_1}{\partial \mathbf{q}} - \frac{\partial h}{\partial \mathbf{q}}\cdot\frac{\partial F_1}{\partial \mathbf{p}} = -\frac{\partial F_0}{\partial \tau_2} \tag{20}$$

Equation (19) is the $\varepsilon^0$-order equation of motion for $F$. It describes the evolution of $F$ under a frozen Hamiltonian $h$. Motion governed by the frozen Hamiltonian is presumed to be ergodic on the surface $h = \text{const}$. Thus, $F_0$ must be constant on surfaces of constant $h$. The solution to Eq. (19) subject to Eq. (13) is thus

$$F_0(\mathbf{p}, \mathbf{q}; \tau_2) = k(\tau_2)\,\delta[h(\mathbf{p}, \mathbf{q}; \tau_2) - E(\tau_2)] \tag{21}$$

where, in order to satisfy the initial condition, $k(0)$ and $E(0)$ are specified, but $k(\tau_2)$ and $E(\tau_2)$ are otherwise undetermined functions of $\tau_2$. In order for the expansion $F = F_0 + \varepsilon F_1$ to be useful, we want to look at times that are of the order of $1/\varepsilon$. To do this, $F_1$ is required to be free from secular time dependences that cause it to grow rapidly to levels $F_1 \sim 1/\varepsilon$ at $t \sim 1/\varepsilon$. Adopting this requirement, it can be shown[11] that the order-$\varepsilon^1$ evolution equation (20) leads to the following equations, giving a unique determination of $k$ and $E$:

$$\frac{d}{d\tau_2} \int k(\tau_2)\, \delta[h(\mathbf{p}, \mathbf{q}; \tau_2) - E(\tau_2)]\, d^N p\, d^N q = 0 \tag{22}$$

$$\frac{d}{d\tau_2} \int U[h(\mathbf{p}, \mathbf{q}; \tau_2) - E(\tau_2)]\, d^N p\, d^N q = 0 \tag{23}$$

Equation (23) expresses the conservation of the adiabatic invariant ($\mu = \text{const}$), while Eq. (22) expresses the conservation of the number of particles [Eq. (22) can also be written $k\, \partial\mu/\partial E = \text{const}$]. These two equations, along with the initial values for $k$ and $E$, determine $k(\tau_2)$ and $E(\tau_2)$.

The $F_0$ given by Eq. (21) gives no contribution to the right-hand side of Eq. (15) [by virtue of the identity $x\, \delta(x) \equiv 0$]. Hence, the solution to Eq. (19) given by Eq. (21) is insufficient by itself to determine an approximation to the dependence of $\langle (\Delta H)^2 \rangle$ on $t$. To determine $\langle (\Delta H)^2 \rangle$, we must look to the $\varepsilon^1$-order term in $F$. With $F_0$ specified by virtue of Eqs. (21)–(23), we can solve Eq. (20) by the method of characteristics to get

$$F_1 = -\int^{\tau_1} \frac{\partial F_0}{\partial \tau_2} (\mathbf{P}(\tau_1^*), \mathbf{Q}(\tau_1^*); \tau_2)\, d\tau_1^* \tag{24}$$

where the integration is over times $\tau_1^* < \tau_1$ and the orbit $\mathbf{P}(\tau_1^*)$ and $\mathbf{Q}(\tau_1^*)$ represent solutions of Hamilton's equations in the frozen Hamiltonian $h(\mathbf{p}, \mathbf{q}; \tau_2)$, which at the time $\tau_1^* = \tau_1$ satisfy the "final condition," $\mathbf{P}(\tau_1) = \mathbf{p}$ and $\mathbf{Q}(\tau_1) = \mathbf{q}$. After inserting Eqs. (24) and (21) into Eq. (15) and reverting back to the $t$ variable, we are able to determine[11] the time dependence of $\langle (\Delta H)^2 \rangle$,

$$\frac{d}{dt} \langle (\Delta H)^2 \rangle = 2 \int_0^t C(s, t)\, ds \tag{25}$$

where $C(s, t)$ is the following autocorrelation function:

$$C(s, t) \equiv \int d^N p\, d^N q\, F_0 \left( \frac{\partial H}{\partial t} - \frac{dE}{dt} \right) O_s(t) \left( \frac{\partial H}{\partial t} - \frac{dE}{dt} \right) \tag{26}$$

In Eq. (26), $O_s(t)$ is an operator that translates values of $\mathbf{p}$ and $\mathbf{q}$ *backward* in time from an initial moment $t$ by an amount $s$ by following the trajectory of the particle in the frozen Hamiltonian $H(\mathbf{p}, \mathbf{q}; \varepsilon t)$.

Equation (26) is the autocorrelation function we discussed in Sections 1 and 2. Its exact value for a particular $H$ will probably be difficult to determine either numerically or theoretically. Here, however, we are primarily interested in how $\langle (\Delta H)^2 \rangle$ scales, and this is easy to determine from Eqs. (25) and (26). First we consider the case where $C(s, t)$ is integrable,

$$\int_0^\infty C(s, t)\, ds < \infty$$

In this case, for large $t \gg \tau_c$ [where $\tau_c$ is the characteristic correlation time in which $C(s, t)$ decreases appreciable with $s$] we have

$$\int_0^t C(s, t)\, ds \simeq \int_0^\infty C(s, t)\, ds$$

Putting this into Eq. (25), we have, for long times $t \sim T$,

$$\langle (\Delta H)^2 \rangle \sim T \int_0^\infty C(s, t)\, ds$$

Due to the time derivatives in the definition of $C(s, t)$, Eq. (26), the integral can be estimated as being of order $H^2 \tau_c / T^2$. Thus, in terms of the scaling with $T$ we have the result

$$\langle (\Delta H)^2 \rangle^{1/2} \sim (1/T)^{1/2} \tag{27}$$

at $t \sim T$. This is the result used for comparison with the numerical experiments, Example 1 of Section 2. Equation (27) can be simply understood as follows. The spread about the $H = E$ surface is basically diffusive due to the chaotic dynamics and the short-time correlations, $\int_0^\infty C(s, t)\, ds < \infty$. Thus, we expect the error to scale as $(DT)^{1/2}$, where $D \equiv \int_0^\infty C(s, t)\, ds$ is the diffusion coefficient. However, $D$ itself is caused by the time variation of the system and scales as $T^{-2}$. Thus, Eq. (27) follows.

Now we consider the case where $\int_0^\infty C(s, t)\, ds = \infty$. Assume that for large $s$ (i.e., sufficiently greater than some value, which we denote $\tau_c$), $s \gg \tau_c$, $C(s, t)$ has a power law dependence on $s$,

$$C(s, t) \sim \frac{H}{T^2} s^{-\xi}, \qquad \xi \leqslant 1$$

We now consider what effect the value of $\xi$ has on the time dependence of the error in $\mu$. For $\xi = 1$ and large $t$, Eq. (25) yields

$$\frac{d}{dt}\langle(\Delta H)^2\rangle \sim \frac{2H^2}{T^2}\ln\frac{t}{\tau_c}$$

If we integrate this equation and let $t \sim T \gg \tau_c$, we get

$$\langle(\Delta H)^2\rangle^{1/2} \sim [(\ln T)/T]^{1/2} \tag{28}$$

This scaling was shown in Section 2 to agree well with the numerical experiment denoted Example 2. For $0 < \xi < 1$, Eq. (25) yields

$$\langle(\Delta H)^2\rangle^{1/2} \sim (1/T)^{\xi/2} \tag{29}$$

in the adiabatic limit. While our Example 3 of Section 2 appears to yield a roughly power law dependence on $T$ as in Eq. (29), this theory does not strictly apply, since hypothesis (a) of Section 1 is not satisfied.

We now turn to the determination of $\langle\Delta H\rangle$. We multiply Eq. (14) by $H - E$ and integrate over all phase space. After an integration by parts, we obtain

$$\frac{d}{dt}\langle\Delta H\rangle = \int F\left(\frac{\partial H}{\partial t} - \frac{dE}{dt}\right) d^N p\, d^N q \tag{30}$$

where $\langle\Delta H\rangle \equiv \int F(H-E)\, d^N p\, d^N q$. If we insert Eqs. (17), (21), and (24) into Eq. (30), we have

$$\frac{d}{dt}\langle\Delta H\rangle = \int F_0\left(\frac{\partial H}{\partial t} - \frac{dE}{dt}\right) d^N p\, d^N q - \int^t dt^* \int d^N p\, d^N q \left(\frac{\partial H}{\partial t} - \frac{dE}{dt}\right)\frac{\partial F_0^*}{\partial t} \tag{31}$$

where $\partial F_0^*/\partial t$ denotes $\partial F_0/\partial t$ with its $(\mathbf{p}, \mathbf{q})$ arguments replaced by $(\mathbf{P}(t^*), \mathbf{Q}(t^*))$ as defined by Eq. (24). From Eq. (23) we see that the first integral on the right-hand side of Eq. (31) is zero. Using Eqs. (23) and (26), we find that Eq. (31) becomes

$$\frac{d}{dt}\langle\Delta H\rangle = \frac{\partial}{\partial E}\int_0^t C(s, t)\, ds \tag{32}$$

where the derivative $\partial/\partial E$ is taken to act only on the $E$ that appears in $F_0 = k\delta[H - E]$ in Eq. (26). Following the same arguments as we applied to Eq. (25), we find that at $t \sim T$ the quantity $\langle\Delta H\rangle$ has the same scaling

with $T$ as does $\langle(\Delta H)^2\rangle$. Namely, for $\int_0^\infty C(s,t)\,ds<\infty$, $\langle\Delta H\rangle\sim T^{-1}$; for $C(s,t)\sim 1/s$, $\langle\Delta H\rangle\sim T^{-1}\ln T$; and for $C(s,t)\sim(1/s)^\xi$, $0<\xi<1$, $\langle\Delta H\rangle\sim T^{-\xi}$. If we compare the deviations from the predicted energy surface due to $\langle(\Delta H)^2\rangle$ and $\langle\Delta H\rangle$, we see that the former is always bigger, $\langle(\Delta H)^2\rangle^{1/2}/\langle\Delta H\rangle\gg 1$, for large $T$,

$$\frac{\langle(\Delta H)^2\rangle^{1/2}}{\langle\Delta H\rangle}\sim\begin{cases}T^{1/2}\\(T^{-1}\ln T)^{-1/2}\\T^{\xi/2}\end{cases}$$

for the three cases, respectively.

Returning now to the adiabatic invariant $\mu$, Eqs. (11) and (12) imply the scalings

$$\langle\Delta\mu\rangle,\ \langle(\Delta\mu)^2\rangle\sim\begin{cases}T^{-1}\\T^{-1}\ln T\\T^{-\xi}\end{cases}\tag{33}$$

for the three cases. In deriving Eqs. (11) and (12), we neglected terms in Eqs. (9) and (10) of order $(\Delta H)^3$ and higher. This is justified if these terms are higher order in $\varepsilon$ than the leading order terms shown in Eq. (33). This will be the case if, when we calculate $\langle(\Delta H)^n\rangle$ $(n\geqslant 3)$ using $F=F_0+\varepsilon F_1$, we obtain $\langle(\Delta H)^n\rangle=0$. This would mean that, to obtain a nonzero result for $\langle(\Delta H)^n\rangle$ $(n\geqslant 3)$, we need to calculate $F$ to order $\varepsilon^2$ at least. The result will be a contribution that is smaller than our leading order term by a factor $O(\varepsilon)$. We now verify that $\langle(\Delta H)^n\rangle$ $(n\geqslant 3)$ satisfies the necessary condition.

We multiply Eq. (14) by $(H-E)^n$ and integrate over all phase space to get

$$\frac{d}{dt}\langle(\Delta H)^n\rangle=\int F(H-E)^{n-1}\left(\frac{\partial H}{\partial t}-\frac{dE}{dt}\right)d^Np\,d^Nq\tag{34}$$

where $\langle(\Delta H)^n\rangle\equiv\int F(H-E)^n\,d^Np\,d^Nq$. If we insert Eqs. (17), (21), and (24) into Eq. (34), we have

$$\frac{d}{dt}\langle(\Delta H)^n\rangle=\int F_0(H-E)^{n-1}\left(\frac{\partial H}{\partial t}-\frac{dE}{dt}\right)d^Np\,d^Nq$$
$$-\int^t dt\int d^Np\,d^Nq\,(H-E)^{n-1}\left(\frac{\partial H}{\partial t}-\frac{dE}{dt}\right)\frac{\partial F_0^*}{\partial t}+O(\varepsilon^3)\tag{35}$$

where $\partial F_0^*/\partial t$ is defined below Eq. (31). From Eq. (21) we see that the integrands in Eq. (35) contain terms of the form $(H-E)\,\delta[H-E]$, which is identically zero. Thus, the solution to Eq. (34) subject to the initial condition (13) yields $\langle(\Delta H)^n\rangle \leqslant O(\varepsilon^2)$.

### 3.2. Analysis for Billiards

A particle incident on a moving wall with velocity $\mathbf{v}_-$ is reflected from the wall with velocity $\mathbf{v}_+$. The reflection law relating $\mathbf{v}_+$ and $\mathbf{v}_-$ is $\mathbf{v}_\pm = \mathbf{v}_\mp \pm 2[\mathbf{w} - (\hat{\mathbf{n}}\cdot\mathbf{v}_\mp)\hat{\mathbf{n}}]$, where we recall that $\mathbf{w}$ is the local wall velocity at the collision point and is normal to the wall, and $\hat{\mathbf{n}}$ is the unit normal outward from the accessible billiard domain. The Liouville equation for billiards is simply Eq. (14) with $H = mv^2/2$:

$$\frac{\partial F}{\partial t} + \mathbf{v}\cdot\frac{\partial F}{\partial \mathbf{x}} = 0 \tag{36}$$

This equation applies inside the billiard. At the walls, $F$ satisfies a boundary condition obtained from the reflection law,

$$F(\mathbf{x}, \mathbf{v}; t) = F(\mathbf{x}, \mathbf{v} + 2[\mathbf{w} - (\hat{\mathbf{n}}\cdot\mathbf{v})\hat{\mathbf{n}}]; t) \tag{37}$$

Our treatment of Eqs. (36) and (37) will follow steps analogous to those we followed in the treatment of the smooth Hamiltonian, Section 3.1. Again we use a two-time-scale expansion. Let

$$\mathbf{w} = \varepsilon\mathbf{u}(\tau_2), \qquad \mathbf{u} = u\hat{\mathbf{n}}$$

$$F = F_0(\mathbf{x}, \mathbf{v}; \tau_2) + \varepsilon F_1(\mathbf{x}, \mathbf{v}; \tau_1, \tau_2)$$

$$\tau_1 = t, \qquad \tau_2 = \varepsilon t$$

The order-$\varepsilon^0$ terms in the expansion of Eqs. (36) and (37) yield

$$\mathbf{v}\cdot\frac{\partial F_0}{\partial \mathbf{x}} = 0$$

inside the billiard, and

$$F_0(\mathbf{x}, \mathbf{v}; \tau_2) = F_0(\mathbf{x}, \mathbf{v} - 2(\hat{\mathbf{n}}\cdot\mathbf{v})\hat{\mathbf{n}}; \tau_2)$$

on the boundary. Due to the assumed ergodic behavior, the solution of these equations for $F_0$ is an arbitrary function of $mv^2/2$. As in Section 3.1, we take as our initial condition $F = F_0 =$ a $\delta$-function on the energy surface. It then follows that

$$F_0 = k(\tau_2)\,\delta[mv^2/2 - E(\tau_2)] \tag{38}$$

where the slow time functions $E(\tau_2)$ and $k(\tau_2)$ are so far arbitrary, except that their initial values $k(0)$ and $E(0)$ are specified.

To find $E(\tau_2)$ and $k(\tau_2)$, we proceed to the order-$\varepsilon$ expansion of Eqs. (36) and (37):

$$\frac{\partial F_1}{\partial \tau_1} + \mathbf{v} \cdot \frac{\partial F_1}{\partial \mathbf{x}} = -\frac{\partial F_0}{\partial \tau_2} \tag{39}$$

$$F_1(\mathbf{x}, \mathbf{v}; \tau_1, \tau_2) - F_1(\mathbf{x}, \mathbf{v} - 2(\hat{\mathbf{n}} \cdot \mathbf{v})\hat{\mathbf{n}}; \tau_1, \tau_2) = (2\hat{\mathbf{n}} \cdot \mathbf{u}) \left( \frac{\partial F_0}{\partial v_n} \right) \tag{40}$$

where $v_n = \mathbf{v} \cdot \hat{\mathbf{n}}$. Multiplying Eq. (39) by $g(mv^2/2)$, an arbitrary function of $mv^2/2$, and integrating over the billiard domain, we obtain

$$-\frac{\partial}{\partial \tau_1} \iint_A F_1 \, g \, dA \, d^2\mathbf{v} = \iint_A \frac{\partial}{\partial \mathbf{x}} \cdot (\mathbf{v} g F_1) \, dA \, d^2\mathbf{v} + \iint_A g \frac{\partial F_0}{\partial \tau_2} \, dA \, d^2\mathbf{v} = 0$$

where we have specialized to the two-dimensional case, $N = 2$, and the integral $\int_A \cdots dA$ is over the accessible billiard area ($dA$ is an area element of the billiard domain). We wish to choose the free functions $k(\tau_2)$ and $E(\tau_2)$ so that the expansion $F \simeq F_0 + \varepsilon F_1$ remains valid for long times, $\tau_2 \sim O(1)$ [i.e., $\tau_1 = t \sim O(1/\varepsilon)$]. To accomplish this, we must ensure that $F_1$ is free of a secular time dependence on $\tau_1$ that would cause $F_1$ to become $O(1/\varepsilon)$ when $\tau_1$ becomes $O(1/\varepsilon)$. Hence we must have

$$\frac{\partial}{\partial \tau_1} \iint_A F_1 \, g \, dA \, d^2\mathbf{v} \equiv 0$$

for any $g$. Thus, we require that

$$\iint_A \left\{ \frac{\partial}{\partial \mathbf{x}} \cdot (\mathbf{v} g F_1) + g \frac{\partial F_0}{\partial \tau_2} \right\} dA \, d^2\mathbf{v} = 0 \tag{41}$$

Making use of the boundary condition (40) and the divergence theorem, we can show that Eqs. (41) and (38) yield

$$\frac{dg(E)}{dE} \left( \frac{dE}{d\tau_2} \iint_A F_0 \, dA \, d^2\mathbf{v} + \oint\!\!\iint \hat{\mathbf{n}} \cdot \mathbf{u} m v_n^2 F_0 \, dl \, d^2\mathbf{v} \right)$$
$$+ g(E) \left( \frac{\partial}{\partial \tau_2} \iint_A F_0 \, dA \, d^2\mathbf{v} \right) = 0 \tag{42}$$

where the integral $\oint \cdots dl$ is over the billiard walls. Since $g$ is an arbitrary

function, the coefficients of $g(E)$ and $dg(E)/dE$ in Eq. (42) must separately be zero. Thus, we obtain the condition

$$\frac{\partial}{\partial \tau_2} \iint_A F_0 \, dA \, d^2\mathbf{v} = 0$$

(which corresponds to particle conservation), and the condition

$$\frac{dE}{d\tau_2} \iint_A F_0 \, dA \, d^2\mathbf{v} + \oint \hat{\mathbf{n}} \cdot \mathbf{u} \int m v_n^2 F_0 \, dl \, d^2\mathbf{v} = 0$$

Making use of the first condition, we can adopt the normalization

$$\iint_A F_0 \, dA \, d^2\mathbf{v} \equiv 1 \tag{43}$$

Making use of Eqs. (38) and (43) and noting that $\oint \hat{\mathbf{n}} \cdot \mathbf{u} \, dl = dA/d\tau_2$, the second condition becomes $dE/d\tau_2 + (E/A)\, dA/d\tau_2 = 0$, or

$$\frac{d}{dt}(EA) = 0 \tag{44}$$

which is the statement of the adiabatic invariant. Equations (43) and (44) ensure the absence of secular behavior and determine the slow time functions $k(\tau_2)$ and $E(\tau_2)$.

We now examine the quantities

$$\frac{d}{dt} \langle (\Delta H)^2 \rangle = \frac{d}{dt} \iint_A \left( \frac{mv^2}{2} - E \right)^2 F \, dA \, d^2\mathbf{v} \tag{45}$$

$$\frac{d}{dt} \langle \Delta H \rangle = \frac{d}{dt} \iint_A \left( \frac{mv^2}{2} - E \right) F \, dA \, d^2\mathbf{v} \tag{46}$$

In Appendix C we manipulate Eqs. (45) and (46) to show that, to lowest significant order in $\varepsilon$, we can express the time derivatives of $\langle (\Delta H)^2 \rangle$ and $\langle \Delta H \rangle$ as

$$\frac{d}{dt} \langle (\Delta H)^2 \rangle \simeq -2 \frac{dE}{dt} \iint_A \left( \frac{mv^2}{2} - E \right) F_1 \, dA \, d^2\mathbf{v} - 4\varepsilon^2 \oint\!\!\iint \left( \frac{mv^2}{2} - E \right) \left( \frac{mv_n^2}{2} \right) (\mathbf{u} \cdot \hat{\mathbf{n}}) \, F_1 \, d^2\mathbf{v} \, dl \tag{47}$$

$$\frac{d}{dt} \langle \Delta H \rangle \simeq \varepsilon^2 \oint\!\!\iint (m v_n^2)(\mathbf{u} \cdot \hat{\mathbf{n}}) \, F_1 \, d^2\mathbf{v} \, dl \tag{48}$$

It remains to determine $F_1$ for insertion into Eqs. (47) and (48).

Unlike the problem for $F_1$ in Section 3.1, we have an inhomogeneous surface term [the right-hand side of Eq. (40)], as well as the previously occurring inhomogeneous volume term [the right-hand side of Eq. (39)]. To solve this problem, we consider the Green's function $G(\mathbf{x}, \mathbf{x}'; \mathbf{v}, \mathbf{v}'; \tau_1 - \tau_1')$, which is the solution of

$$\frac{\partial G}{\partial \tau_1} + \mathbf{v} \cdot \frac{\partial G}{\partial \mathbf{x}} = \delta(\mathbf{x} - \mathbf{x}')\, \delta(\mathbf{v} - \mathbf{v}')\, \delta(\tau_1 - \tau_1') \tag{49}$$

$$G(\mathbf{x}, \mathbf{x}'; \mathbf{v}, \mathbf{v}'; \tau_1 - \tau_1') = G(\mathbf{x}, \mathbf{x}'; \mathbf{v} - 2(\hat{\mathbf{n}} \cdot \mathbf{v})\hat{\mathbf{n}}, \mathbf{v}'; \tau_1 - \tau_1') \tag{50}$$

where the second condition applies if $\mathbf{x}$ is on the billiard boundary and $G \equiv 0$ for $\tau_1 < \tau_1'$. The right-hand side of Eq. (49) represents the creation of a particle at the instant $\tau_1 = \tau_1'$ at the point $\mathbf{x} = \mathbf{x}'$ with velocity $\mathbf{v} = \mathbf{v}'$. Thus, setting $s = \tau_1 - \tau_1'$, we have

$$G = \delta[\mathbf{x} - \mathbf{X}(\mathbf{x}', \mathbf{v}' \mid s)]\, \delta[\mathbf{v} - \mathbf{V}(\mathbf{x}', \mathbf{v}' \mid s)]\, U[s] \tag{51}$$

where $\mathbf{X}(\mathbf{x}', \mathbf{v}' \mid s)$ and $\mathbf{V}(\mathbf{x}', \mathbf{v}' \mid s)$ are particle orbits (with the billiard shape frozen at $t = \tau_2/\varepsilon$), which satisfy the initial conditions (i.e., $s = 0$),

$$\mathbf{X}(\mathbf{x}', \mathbf{v}' \mid 0) = \mathbf{x}', \qquad \mathbf{V}(\mathbf{x}', \mathbf{v}' \mid 0) = \mathbf{v}' \tag{52}$$

By time reversal $G$ can also be expressed in the alternate form

$$G = \delta[\mathbf{x}' - \mathbf{X}(\mathbf{x}, \mathbf{v} \mid -s)]\, \delta[\mathbf{v}' - \mathbf{V}(\mathbf{x}, \mathbf{v} \mid -s)]\, U[s] \tag{53}$$

By conservation of energy in the frozen billiard,

$$\tfrac{1}{2}m\mathbf{V}^2(\mathbf{x}', \mathbf{v}' \mid s) = \tfrac{1}{2}m\mathbf{v}'^2 \tag{54}$$

In terms of $G$, the solution to Eqs. (39) and (40) is

$$F_1 = -\int_0^\infty \left[ \iint_A \left( \frac{\partial F_0'}{\partial \tau_2} \right) G\, d\mathbf{x}'\, d\mathbf{v}' - \oint\!\!\!\!\!\!\iint \hat{\mathbf{n}} \cdot \mathbf{u}(l') \left( \frac{\partial F_0'}{\partial \mathbf{v}_n'} \right) G v_n'\, dl'\, d\mathbf{v}' \right] ds \tag{55}$$

where $F_0' \equiv F_0(\mathbf{x}', \mathbf{v}'; \tau_2)$ and the integral $\oint$ is defined so that it is done just inside the billiard boundary by an infinitesimal amount (we need to make such a definition because $\mathbf{V}$ changes discontinuously on reflection and so is not defined on the walls). Consider the volume integral in Eq. (55); by Eq. (53) we may replace $\mathbf{v}'$ in $F_0'$ by $\mathbf{V}(\mathbf{x}, \mathbf{v} \mid -s)$; and, since $F_0'$ depends on $\mathbf{v}'$ only through $\frac{1}{2}m\mathbf{v}'^2 \to \frac{1}{2}m\mathbf{V}^2(\mathbf{x}, \mathbf{v} \mid -s) = \frac{1}{2}mv^2$ [by Eq. (54)], we can remove the prime from $F_0'$. This allows us to take $\partial F_0/\partial \tau_2$ outside the integrals over $\mathbf{x}'$ and $\mathbf{v}'$. Thus, the first integral in Eq. (55) becomes just $\partial F_0/\partial \tau_2$, where we have noted that $\iint_A G\, d\mathbf{x}'\, d\mathbf{v}' = U[s]$ from Eq. (53). We

now make use of Eqs. (38), (43), and (44) and the identity $\delta(x) = -x\delta'(x)$ to write

$$\partial F_0/\partial \tau_2 = -mv^2/2(A^{-1}\,\partial A/\partial \tau_2)\,\partial F_0/\partial E$$

Also, we note that $\partial F_0/\partial v_n = -mv_n\,\partial F_0/\partial E$. Equation (55) thus becomes

$$F_1 = \int_0^\infty ds \frac{\partial F_0}{\partial E}\left[\frac{mv^2}{2} A^{-1}\frac{\partial A}{\partial \tau_2} + \oint\!\!\oint \hat{\mathbf{n}}\cdot\mathbf{u}(l')\, mv_n'^2 G\, dl'\, d\mathbf{v}'\right] \tag{56}$$

Substituting Eq. (56) into Eq. (47) and making use of Eq. (38) and $\partial A/\partial \tau_2 = \oint \hat{\mathbf{n}}\cdot\mathbf{u}(l')\, dl'$, we again obtain Eq. (25), but with the correlation function now given by

$$C(s,t) = \oint\!\!\oint\!\!\int\!\!\int F_0\left[(mv_n^2)(mv_n'^2)G - E^2\frac{\delta(\mathbf{v}-\mathbf{v}')}{A}\right] \times [\mathbf{w}(l)\cdot\hat{\mathbf{n}}][\mathbf{w}(l')\cdot\hat{\mathbf{n}}]\, d^2\mathbf{v}\, d^2\mathbf{v}'\, dl\, dl' \tag{57}$$

Similar steps yield Eq. (32) for $d\langle \Delta H\rangle/dt$. Thus, proceeding as in Section 3.1, we conclude that the scalings with $T$ derived for smooth Hamiltonians [Eqs. (27)–(29)] also apply for billiards.

## 4. CONCLUSIONS

In conclusion, we can summarize our main results as follows:

1. For slowly time-dependent systems whose orbits in their frozen Hamiltonian ergodically fill the energy surface, the quantity $\mu$ defined by Eq. (1) is an adiabatic invariant.

2. In terms of the correlation function $C(s, t)$ defined in Eq. (26) or Eq. (57), three cases have been treated theoretically, with the following results for the scaling with $T$ of $\langle(\Delta\mu)^2\rangle$ and $\langle\Delta\mu\rangle$ evaluated at $t \sim T$:

(a) If $\int_0^\infty C(s,t)\, ds < \infty$, then $\langle(\Delta\mu)^2\rangle$ and $\langle\Delta\mu\rangle$ scale as $T^{-1}$.

(b) If $C(s, t)$ has a long-time $1/s$ tail, then $\langle(\Delta\mu)^2\rangle$ and $\langle\Delta\mu\rangle$ scale as $T^{-1}\ln T$.

(c) If $C(s, t)$ has a long-time $(1/s)^\xi$ tail with $0 < \xi < 1$, then $\langle(\Delta\mu)^2\rangle$ and $\langle\Delta\mu\rangle$ scale as $T^{-\xi}$.

3. The scalings (a) and (b) above have been tested numerically using billiards. The results agree well with the theoretical predictions.

4. Numerical experiments have been done on a system for which orbits generated by the frozen Hamiltonian are not completely ergodic on

the energy surface, but, except for small island regions, do sample most of the energy surface. In this case the ergodic adiabatic invariant is less well conserved than in the other examples. In particular, $\langle(\Delta\mu)^2\rangle$ scales roughly as $T^{-\xi}$ with $\xi$ substantially less than one. [Although this is also the case for (c) above, the theory does not apply here, since orbits are not ergodic on the energy surface.] A brief preliminary version of this work appears in Ref. 21.

## APPENDIX A. ENTROPY AND QUANTUM CHAOS

In this Appendix we offer some additional tangential remarks concerning the ergodic adiabatic invariant. In particular, we discuss its relationship to the concept of entropy, and we also discuss its implications for the variation of quantum energy level spectra in the quasiclassical limit (small $\hbar$) for systems whose classical behavior is chaotic.

*Entropy.* The entropy is commonly written as (Ref. 10, p. 11)

$$S = \log[\Omega(E)] + \text{const} \tag{A1}$$

where $\Omega(E)$ is the area of the energy hypersurface,

$$\Omega(E) = \iint \delta(H - E)\, d^N p\, d^N q$$

In terms of the ergodic invariant we can also write $\Omega(E) = \partial\mu/\partial E$. The number of states of energy less than $E$ is approximately

$$\iint U[E - H]\, d^N p\, d^N q/h^N = \mu/h^N$$

where $h$ is Planck's constant. For large $N$

$$\log \Omega \simeq \log \mu \tag{A2}$$

That is, for large dimensionality, the logarithm of the surface and the logarithm of the volume are approximately equal (e.g., this is easily seen in the case of an $N$-dimensional sphere of radius $r$, for which surface area $\sim r^{N-1}$ and volume $\sim r^N$). Thus, the ergodic adiabatic invariant is closely related to the concept of entropy when $N$ is large. In particular, by Eq. (A2), the constancy of entropy during an adiabatic gas transformation implies constancy of $\log \mu$ (in the $N \to \infty$ limit). This shows why (as noted in Section 1) setting $\mu = \text{const}$ for a single particle yields a condition analogous to the adiabatic gas law (which is a many-particle, i.e., large-$N$, result).

*Quantum Chaos.* The field of study that attempts to explore the semiclassical (small-$\hbar$) behavior of a quantum system whose classical counterpart is chaotic is called quantum chaos. One of the results in quantum chaos is that for classically chaotic systems (without symmetries), as a parameter of the system is varied, energy levels of the corresponding quantum system avoid crossing each other, as illustrated in Fig. 9a. For separable systems, such as a rectangular box, this is not the case (e.g., Fig. 9b). Say we initialize a quantum system in a state with energy level $E_n$. We then have the system evolve forward in time by slowly changing the Hamiltonian. Suppose energy level crossings are avoided for this system. Then, for very slow time variation, the system will remain in the state that is homotopic to its initial state [denote the energy of this state $E(t)$, $E(0)=E_n$]. Furthermore, since energy level crossings are avoided, $\hat{N}(E(T))$, the number of states with energies less than $E(t)$, is constant in time. For example, in Fig. 9c the energy level curves can be labeled in order of increasing energy (e.g., $E_{n-1}<E_n<E_{n+1}<E_{n+2}$ for all values of the parameter). Since $\hat{N}(E)\simeq \mu/h^N$, we can now state the following:

*The quantum version of the ergodic adiabatic invariant of classical mechanics is the avoidance of quantum energy level crossings for classically chaotic systems.*

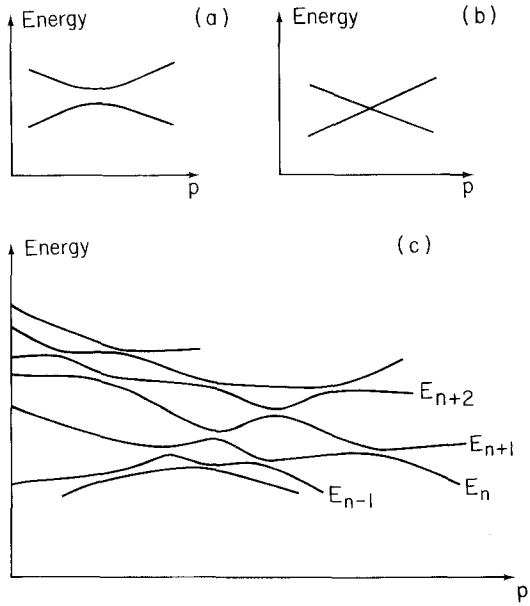


Fig. 9. Energy level versus a system parameter $p$. (a) Avoided energy level crossing for a chaotic system. (b) Energy levels cross in a separable system. (c) Several energy levels and avoided crossings in a chaotic system.

We thank T. M. Antonsen for discussion leading to the above remark. See also discussion by Berry,[19] who previously noted the relevance of the ergodic adiabatic invariant for quantum chaos energy level spectra.

## APPENDIX B. CALCULATION OF μ

We consider here the explicit calculation of $\mu$, defined by Eq. (1), for $N=2$. We write $d^2p$ in polar coordinates as $d^2p = p\,dp\,d\phi$. With $H = \mathbf{p}\cdot\mathbf{p}/2m + V(\mathbf{q}; t)$,

$$\mu(E, t) = \int d^2q \int_0^{2\pi} d\phi \int_0^{\infty} p\,dp\; U[E - (p^2/2m) - V(\mathbf{q}; t)]$$

Using the change of variables $\chi \equiv p^2/2m$, we have $p\,dp = m\,d\chi$. Performing the $\chi$ and $\phi$ integration yields

$$\mu(E, t) = 2\pi m \int (E - V)\, U[E - V]\, d^2q \tag{B1}$$

For billiards integrate $d^2q$ only over the confining region where $V=0$, since the particle has zero probability of escaping the confining region. Thus,

$$\mu(E, t) = 2\pi m E A$$

For Example 3 the potential is

$$V = g(t)\, x^2 + y^2 + x^2y^2$$

Performing the $x$ integration, we have that Eq. (B1) becomes

$$\mu(E, t) = \frac{8\pi m}{3} \int_{-\beta}^{\beta} \frac{g^{3/2}(\beta^2 - y^2)^{3/2}}{(1 + y^2)^{1/2}}\, dy \tag{B2}$$

where $\beta^2 \equiv E/g$. Letting $y \equiv \beta \cos\theta$, we find for Eq. (B2)

$$\mu(E, t) = \frac{8\pi m E^2}{3(g + E)^{1/2}} \int_0^{\pi} d\theta\, \frac{\sin^4\theta}{(1 - k^2 \sin^2\theta)^{1/2}}$$

where $k^2 \equiv E/(g + E)$. This is an elliptic integral, which, for $k < 1$, yields,[20]

$$\mu(E, t) = \frac{16\pi m(g + E)^{1/2}}{9} [(3E + 2g)\, F(k) - (4E + 2g)\, K(k)] \tag{B3}$$

where $F$ and $K$ are complete elliptic integrals of the first and second kind, respectively. Thus, we have verified Eq. (8).

## APPENDIX C. DERIVATION OF EQUATION (47)

In this Appendix we show how Eq. (47) is obtained from Eq. (45). The derivation of Eq. (48) from Eq. (46) is similar and is omitted. Differentiating the integral in Eq. (45), we have

$$\frac{d}{dt}\langle(\Delta H)^2\rangle = -2\left(\iint_A \left(\frac{mv^2}{2}-E\right) F\, dA\, d^2\mathbf{v}\right)\frac{dE}{dt} + \iint_A \left(\frac{mv^2}{2}-E\right)^2 \frac{\partial F}{\partial t}\, dA\, d^2\mathbf{v} + \oint\!\!\iint \left(\frac{mv^2}{2}-E\right)^2 (\mathbf{w}\cdot\hat{\mathbf{n}})\, F\, d^2\mathbf{v}\, dl$$

From Eq. (36)

$$\frac{d}{dt}\langle(\Delta H)^2\rangle = -2\frac{dE}{dt}\iint_A \left(\frac{mv^2}{2}-E\right) F\, dA\, d\mathbf{v} - \iint_A \left(\frac{mv^2}{2}-E\right)^2 \left(\mathbf{v}\cdot\frac{\partial F}{\partial \mathbf{x}}\right) d^2\mathbf{v}\, dA + \oint\!\!\iint \left(\frac{mv^2}{2}-E\right)^2 (\mathbf{w}\cdot\hat{\mathbf{n}}) F\, d^2\mathbf{v}\, dl$$

Thus,

$$\frac{d}{dt}\langle(\Delta H)^2\rangle = \frac{dE}{dt}\iint_A \left(\frac{mv^2}{2}-E\right) F\, dA\, d\mathbf{v} - I \tag{C1}$$

where

$$I \equiv \oint\!\!\iint (mv^2/2-E)^2[\hat{\mathbf{n}}\cdot(\mathbf{v}-\mathbf{w})] F\, d^2\mathbf{v}\, dl \tag{C2}$$

We now make a change of integration variables in Eq. (C2) from $\mathbf{v}$ to $\mathbf{v}'$, where

$$\mathbf{v}' \equiv \mathbf{v} + 2[\mathbf{w} - (\hat{\mathbf{n}}\cdot\mathbf{v})\hat{\mathbf{n}}]$$

By virtue of the boundary condition (37), we have $F(\mathbf{x}, \mathbf{v}; t) = F(\mathbf{x}, \mathbf{v}'; t)$ in the integral. $I$ becomes

$$I = -\oint\!\!\iint \{(m\mathbf{v}'^2/2-E)^2 - 4m(\hat{\mathbf{n}}\cdot\mathbf{w})(m\mathbf{v}'^2/2-E)[\hat{\mathbf{n}}\cdot(\mathbf{v}'-\mathbf{w})] + 4m^2(\hat{\mathbf{n}}\cdot\mathbf{w})^2[(\mathbf{v}'-\mathbf{w})\cdot\hat{\mathbf{n}}]^2\}[\hat{\mathbf{n}}\cdot(\mathbf{v}'-\mathbf{w})] F\, d^2\mathbf{v}\, dl$$

The contribution to the right-hand side from the first term in the square brackets is just $-I$. Thus, we have that

$$2I = 4 \oint\!\!\int m(\hat{\mathbf{n}} \cdot \mathbf{w})(mv^2/2 - E)[\hat{\mathbf{n}} \cdot (\mathbf{v} - \mathbf{w})]^2 F \, d^2\mathbf{v} \, dl + 4I'$$

where

$$I' = m^2 \oint\!\!\int (\hat{\mathbf{n}} \cdot \mathbf{w})^2[\hat{\mathbf{n}} \cdot (\mathbf{v} - \mathbf{w})]^3 F \, d^2\mathbf{v} \, dl$$

Making the change of variables from $\mathbf{v}$ to $\mathbf{v}'$ in the above expression for $I'$ gives $I' = -I'$ [since $\hat{\mathbf{n}} \cdot (\mathbf{v} - \mathbf{w}) = -\hat{\mathbf{n}} \cdot (\mathbf{v}' - \mathbf{w})$], or $I' = 0$. Thus

$$I = 2 \oint\!\!\int m(\hat{\mathbf{n}} \cdot \mathbf{w})(mv^2/2 - E)[\hat{\mathbf{n}} \cdot (\mathbf{v} - \mathbf{w})]^2 F \, d^2\mathbf{v} \, dl \tag{C3}$$

Since $x \, \delta(x) \equiv 0$, $F_0$ makes no contribution to $I$. Hence, to lowest significant order, we may replace $F$ by $\varepsilon F_1$ in Eq. (C3). Equation (47) follows from Eqs. (C1)–(C3).

## ACKNOWLEDGMENTS

We thank T. M. Antonsen and J. R. Dorfman for helpful discussions. This work was supported by the Office of Naval Research.

## REFERENCES

1. M. Jammer, *The Conceptual Development of Quantum Mechanics* (McGraw-Hill, 1966), pp. 96–97.
2. A. Lenard, *Ann. Phys. (N.Y.)* **6**:261 (1959).
3. C. S. Gardner, *Phys. Rev.* **115**:791 (1959).
4. M. D. Kruskal, in *Plasma Physics* (International Atomic Energy Agency, 1965).
5. R. Kulsrud, *Phys. Rev.* **106**:205 (1957).
6. T. G. Northrop, *The Adiabatic Motion of Charged Particles* (Interscience, 1963).
7. M. N. Rosenbluth and C. L. Longmire, *Ann. Phys.* **1**:120 (1957).
8. T. M. Antonsen, Jr. and Y. C. Lee, *Phys. Fluids* **25**:132 (1982).
9. P. Ehrenfest, *Phil. Mag.* **33**:500 (1917) [reprinted in B. L. van der Waerden, ed., *Sources of Quantum Mechanics* (Dover, 1967)].
10. R. Kubo, *Statistical Mechanics* (North-Holland, Amsterdam, 1965), p. 14.
11. E. Ott, *Phys. Rev. Lett.* **24**:1628 (1979).
12. H. Goldstein, *Classical Mechanics* (Addison-Wesley, 1959), p. 250.
13. R. V. Lovelace, *Phys. Fluids* **22**:542 (1979).
14. A. Y. Wong, Y. Nakamura, B. H. Quon, and J. M. Dawson, *Phys. Rev. Lett.* **35**:1156 (1975).

15. Ya. G. Sinai, *Russ. Math. Surv.* **25**:137 (1970).
16. A. Zacherl, T. Geisel, J. Nierwetberg, and G. Radons, *Phys. Lett. A* **114**:317 (1986).
17. G. Casati, G. Comparin, and I. Guarneri, *Phys. Rev. A* **26**:717 (1982).
18. A. Carnegie and I. C. Percival, *J. Phys. A: Math. Gen.* **17**:801 (1984).
19. M. V. Berry, in *Theoretical and Applied Mechanics* (Elsevier, 1985).
20. I. S. Gradshteyn and I. M. Ryzhik, *Table of Integrals, Series, and Products* (Academic Press, 1980), p. 162.
21. R. Brown, E. Ott, and C. Grebogi, *Phys. Rev. Lett.* **59**:1173 (1987).